

On the enumeration of integer tetrahedra

James East^{1,2} Michael Hendriksen^{3,4} Laurence Park¹

Abstract

We consider the problem of enumerating integer tetrahedra of fixed perimeter (sum of side-lengths) and/or diameter (maximum side-length), up to congruence. As we will see, this problem is considerably more difficult than the corresponding problem for triangles, which has long been solved. We expect there are no closed-form solutions to the tetrahedron enumeration problems, but we explore the extent to which they can be approached via classical methods, such as orbit enumeration. We also discuss algorithms for computing the numbers, and present several tables and figures that can be used to visualise the data. Several intriguing patterns seem to emerge, leading to a number of natural conjectures. The central conjecture is that the number of integer tetrahedra of perimeter n , up to congruence, is asymptotic to n^5/C for some constant $C \approx 229000$.

Keywords: Enumeration, integer tetrahedra, perimeter, orbit enumeration.

MSC: 52B05, 05A17, 05E18, 05A10.

Contents

1	Introduction	1
2	Enumeration via Burnside's Lemma	3
3	Computation and data	8
4	Observations from the data	11
5	Conclusion	24

1 Introduction

Geometry and combinatorics have many natural meeting points. Arguably the most ancient known example is the application of right-angled integer triangles in Babylonian architecture and agriculture. The classification of all such right triangles is recorded in Book X of Euclid's Elements. Enumeration of arbitrary integer triangles goes back at least to the 1979 paper of Jordan, Walch and Wisner [11], and we have the following elegant result of Honsberger [8], which has been proved in a variety of ways [4–8, 10]:

Theorem. *The number of integer triangles with perimeter n , up to congruence, is the nearest integer to $\frac{n^2}{48}$ if n is even, or to $\frac{(n+3)^2}{48}$ if n is odd.*

Two of the most natural extensions of this triangle enumeration problem are to consider integer polygons (increasing the number of sides), or integer tetrahedra (moving up a dimension). The former was treated in [4], and the current article considers the latter. Our main guiding problem is the following. By an *integer tetrahedron* we mean a (non-degenerate) tetrahedron whose sides are all of integer length, as in Figure 1. The *perimeter* of a tetrahedron is the sum of its six side-lengths.

¹Centre for Research in Mathematics and Data Science, Western Sydney University, Australia. J.East@WesternSydney.edu.au, L.Park@WesternSydney.edu.au.

²Supported by ARC Future Fellowship FT190100632.

³School of Mathematics and Statistics, University of Melbourne, Australia. michael.hendriksen@unimelb.edu.au.

⁴Parts of this research were carried out when this author was a postgraduate student at Western Sydney University, and a postdoctoral fellow at Heinrich Heine Universität Düsseldorf.

Problem 1. Calculate the number t_n of integer tetrahedra with perimeter n , up to congruence: i.e., combinations of rotations, translations and reflections.

One might hope that t_n is given by a similar formula to the triangle sequence in Honsberger's Theorem above. As we will see, however, this is *very* far from the truth.

Philip Benjamin has computed t_n for $n \leq 30$, but as far as we know has not published his methods; see [1, Sequence A208454]. Sascha Kurz [12] has considered the related problem of enumeration by *diameter*, defined to be the maximum of the six side-lengths:

Problem 2. Calculate the number ${}^d t$ of integer tetrahedra with diameter d , up to congruence.

Kurz has computed ${}^d t$ for $d \leq 1000$ in [12]; see also [1, Sequence A097125]. The article [12] gives a lot of detail about Kurz's methods and algorithms. No formula is given or conjectured, though an exact expression is given for a related set of (orbits of) matrices; this leads to a conjectural asymptotic formula, as we discuss in Sections 4.1 and 4.5.

It is not hard to show that the number of integer triangles with diameter d , up to congruence, is equal to $\lfloor \frac{(d+1)^2}{4} \rfloor$; see [1, Sequence A002620].

There is also of course the following natural problem, combining perimeter and diameter:

Problem 3. Calculate the number ${}^d t_n$ of integer tetrahedra with perimeter n and diameter d , up to congruence.

Clearly a solution to Problem 3 would yield solutions to Problems 1 and 2, since

$$t_n = \sum_d {}^d t_n \quad \text{and} \quad {}^d t = \sum_n {}^d t_n.$$

The non-zero terms in these sums occur for $\lceil \frac{n}{6} \rceil \leq d \leq \lfloor \frac{n-3}{3} \rfloor$ and $3d + 3 \leq n \leq 6d$, as we will show in Lemma 3.2.

Apart from this introduction, and a brief conclusion, the paper contains three further sections. In Section 2 we set up some ideas that (in principle) allow the calculation of t_n , ${}^d t$ and ${}^d t_n$ via Burnside's Lemma, and we make some partial progress by giving explicit formulas for some of the relevant parameters. In Section 3 we discuss algorithms for computing the numbers t_n , ${}^d t$ and ${}^d t_n$, and give several tables and graphs of computed values; more data can be found at [3]. In Section 4 we explore some intriguing patterns that seem to emerge from an examination of the data. A number of conjectures/open problems are stated. We hope that these provide inspiration for future studies.

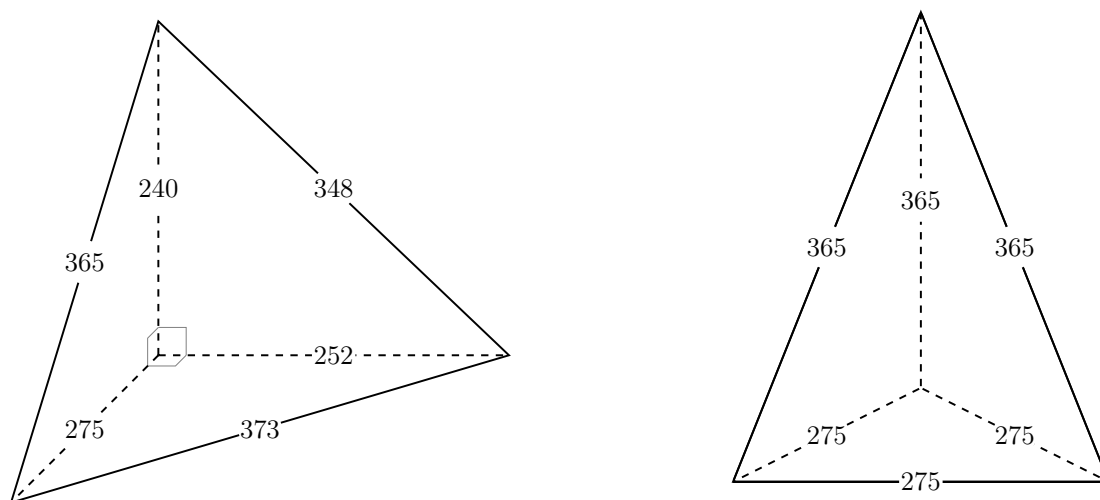


Figure 1. Two integer tetrahedra. The one on the left is tri-rectangular. The one on the right is invariant under a 120° rotation about a vertical axis.

2 Enumeration via Burnside's Lemma

In this section we focus on the numbers t_n , though all we say can easily be adapted to work for the numbers ${}^d t$ or ${}^d t_n$ instead. In Remark 2.13 we indicate the modifications needed for these.

Let \mathcal{G} be the set of all edge-labelled graphs whose underlying unlabelled graph is the complete graph on vertex set $\{1, 2, 3, 4\}$, and whose labels all belong to $\mathbb{N} = \{1, 2, 3, \dots\}$. For $G \in \mathcal{G}$, we denote the label of the edge $\{i, j\}$ by $G(i, j) = G(j, i)$. The symmetric group \mathcal{S}_4 has a natural action on \mathcal{G} , denoted $(\sigma, G) \mapsto \sigma \cdot G$, and induced by permuting the vertices. For $G \in \mathcal{G}$ and $\sigma \in \mathcal{S}_4$, and for distinct $i, j \in \{1, 2, 3, 4\}$, we have

$$(\sigma \cdot G)(i, j) = G(\sigma^{-1}(i), \sigma^{-1}(j)). \quad (2.1)$$

For example, Figure 2 illustrates the action of the permutations $(2, 3)$, $(1, 2, 3)$, $(1, 2, 4, 3)$ and $(1, 4)(2, 3)$, written in standard cycle notation.

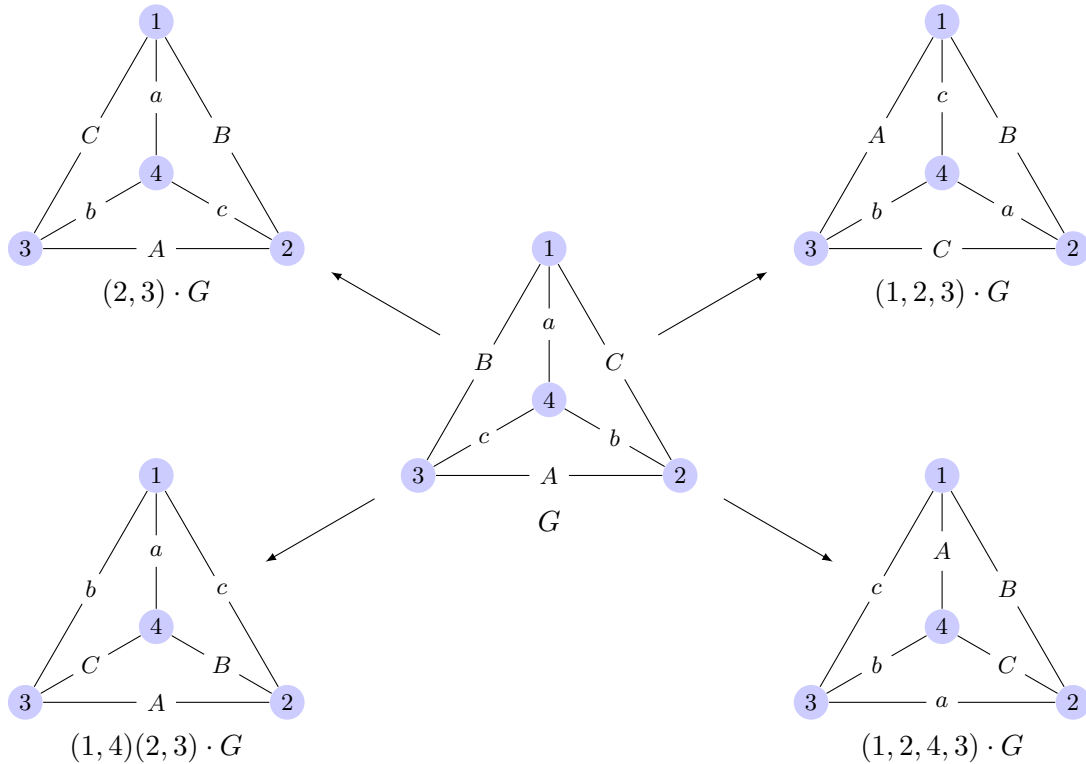


Figure 2. The graph $G \in \mathcal{G}$ (centre), as well as $\sigma \cdot G$ for various permutations σ from \mathcal{S}_4 .

An integer tetrahedron T may be represented by a graph G from \mathcal{G} as follows. Choose an ordering $1, 2, 3, 4$ on the corners of T , and let the label of the edge $\{i, j\}$ from G be the corresponding side-length from T . Different orderings on the vertices typically lead to different graphs, so that T may be represented by up to 24 such graphs. In fact, these graphs representing T are precisely those belonging to the orbit of G under the action of \mathcal{S}_4 given in (2.1). For example, the tetrahedra from Figure 1 may be represented by the graphs in Figure 3; the orbits of these graphs have size 24 and 4, respectively. It is clear that two tetrahedra are congruent if and only if they are represented by the same set of graphs from \mathcal{G} .

Not every graph from \mathcal{G} corresponds to a tetrahedron in the above manner. For example, we claim that this is the case for the two graphs pictured in Figure 4. This is clear for the left-hand graph, as there is no triangle with edges $(1, 1, 2)$. However, the right-hand graph cannot be ruled out so easily, as the triples $(7, 7, 7)$ and $(7, 4, 4)$ do indeed correspond to triangles. Rather, the problem here is that if one tries to fold the “net” shown in Figure 5 (left) into a tetrahedron, then the tips of the three $(7, 4, 4)$ triangles do not meet.

For $n \in \mathbb{N}$, let \mathcal{T}_n be the set of graphs from \mathcal{G} corresponding to some tetrahedron of perimeter n . The

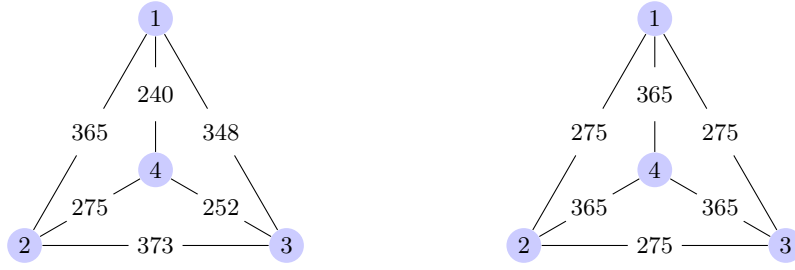


Figure 3. Graphs from \mathcal{G} representing the tetrahedra pictured in Figure 1.

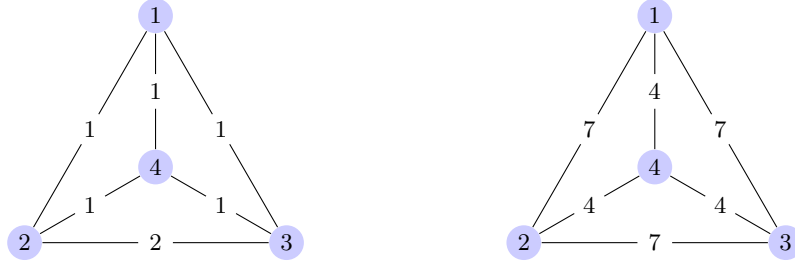


Figure 4. Graphs from \mathcal{G} not corresponding to tetrahedra.

number of integer tetrahedra of perimeter n , up to congruence, is then given by the number $t_n = |\mathcal{T}_n/\mathcal{S}_4|$ of orbits of \mathcal{T}_n under the action of \mathcal{S}_4 given in (2.1). Burnside's Lemma (cf. [2, p. 246]) then gives

$$t_n = |\mathcal{T}_n/\mathcal{S}_4| = \frac{1}{24} \sum_{\sigma \in \mathcal{S}_4} \text{fix}(\sigma). \quad (2.2)$$

Here, for $\sigma \in \mathcal{S}_4$, $\text{fix}(\sigma)$ is the cardinality of the set

$$\text{Fix}(\sigma) = \{G \in \mathcal{T}_n : \sigma \cdot G = G\}. \quad (2.3)$$

To enumerate tetrahedra up to rotations and translations only, we would be looking at orbits under the restricted action of the alternating group $\mathcal{A}_4 \subseteq \mathcal{S}_4$, since even and odd permutations correspond to rotations and reflections, respectively. The number t'_n of integer tetrahedra of perimeter n , up to this kind of restricted congruence, is given by

$$t'_n = |\mathcal{T}_n/\mathcal{A}_4| = \frac{1}{12} \sum_{\sigma \in \mathcal{A}_4} \text{fix}(\sigma). \quad (2.4)$$

Thus, to calculate the numbers t_n and t'_n , it is enough to identify the set \mathcal{T}_n , and calculate the parameters $\text{fix}(\sigma)$ for each $\sigma \in \mathcal{S}_4$. For the former, we have the following:

Proposition 2.5. *The set \mathcal{T}_n consists of all graphs G from \mathcal{G} whose edge-labels, as shown in Figure 2 (centre), satisfy:*

(T1) $A + B + C + a + b + c = n,$

(T2) $A + B + C > 2 \max(A, B, C),$

(T3) $A + b + c > 2 \max(A, b, c),$

(T4) $a + B + c > 2 \max(a, B, c),$

(T5) $a + b + C > 2 \max(a, b, C),$

(T6) $(a^2 - B^2 - c^2 + 2x_1x_2)^2 < 4Y_1Y_2,$ where

- $x_1 = \frac{A^2+B^2-C^2}{2A},$

- $x_2 = \frac{A^2+c^2-b^2}{2A}.$

- $Y_1 = B^2 - x_1^2,$

- $Y_2 = c^2 - x_2^2.$

Proof. First note that three positive real numbers x, y, z can be the sides of a triangle if and only if the sum of the smaller two is greater than the largest; this is equivalent to $x + y + z > 2 \max(x, y, z).$

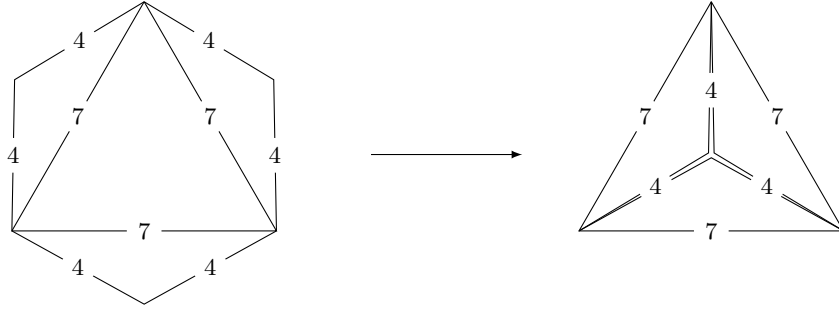


Figure 5. Attempting to construct a tetrahedron from the graph in Figure 4 (right).

Thus, consulting Figure 2, it is clear that \mathcal{T}_n is a subset of

$$\mathcal{T}'_n = \{G \in \mathcal{G} : \text{(T1)–(T5) hold}\}.$$

Now consider a graph G from \mathcal{T}'_n , with edges labelled as in Figure 2. Then G corresponds to a tetrahedron if and only if the following procedure can be carried out:

- Begin with the quadrilateral shown in Figure 6 (left).
- Keeping the (A, B, C) -triangle fixed in place, fold along the x -axis by some angle $0 < \theta < \pi$ until the free tips of the two triangles are a units apart, as shown in Figure 6 (middle). (We have strict inequalities for θ to ensure that the tetrahedron is not degenerate.)

Figure 6 (right) displays the two original triangles, as well as the result of folding by the angle $\theta = \pi$, and defines three points, $P, Q, R \in \mathbb{R}^2$. Let the coordinates of these points be $P = (x_1, y_1)$, $Q = (x_2, y_2)$ and $R = (x_2, -y_2)$. Also, put $Y_1 = y_1^2$ and $Y_2 = y_2^2$. It is easy to check that x_1, x_2, Y_1, Y_2 are as given in (T6): e.g., consider P as the intersection of the circles $x^2 + y^2 = B^2$ and $(x - A)^2 + y^2 = C^2$.

We claim that the above folding procedure can be carried out if and only if $|PQ| < a < |PR|$. Indeed, if we denote by $R_\theta \in \mathbb{R}^3$ the tip of the moving triangle after folding by the angle $0 \leq \theta \leq \pi$, then $R_\theta = (x_2, -y_2 \cos \theta, y_2 \sin \theta)$. It follows that $|PR_\theta|^2 = (x_1 - x_2)^2 + y_1^2 + y_2^2 + 2y_1y_2 \cos \theta$ is a smooth, decreasing function of $0 \leq \theta \leq \pi$.

With the claim established, it remains to observe that the inequality $|PQ| < a < |PR|$ is equivalent to that in (T6), as

$$\begin{aligned} |PQ| < a < |PR| &\Leftrightarrow |PQ|^2 < a^2 < |PR|^2 \\ &\Leftrightarrow (x_1 - x_2)^2 + (y_1 - y_2)^2 < a^2 < (x_1 - x_2)^2 + (y_1 + y_2)^2 \\ &\Leftrightarrow y_1^2 + y_2^2 - 2y_1y_2 < a^2 - (x_1 - x_2)^2 < y_1^2 + y_2^2 + 2y_1y_2 \\ &\Leftrightarrow -2y_1y_2 < a^2 - (x_1 - x_2)^2 - y_1^2 - y_2^2 < 2y_1y_2 \\ &\Leftrightarrow (a^2 - (x_1 - x_2)^2 - y_1^2 - y_2^2)^2 < 4y_1^2y_2^2 \\ &\Leftrightarrow (a^2 - B^2 - c^2 + 2x_1x_2)^2 < 4y_1^2y_2^2. \quad \square \end{aligned}$$

Remark 2.6. Items (T4) and (T5) from Proposition 2.5 are actually unnecessary. Indeed, given (T1)–(T3), and in the notation of the above proof (cf. Figure 6), (T6) is equivalent to the inequality $|PQ| < a < |PR|$. This ensures that the triples (a, B, c) and (a, b, C) correspond to triangles, which implies (T4) and (T5).

Alternative formulations of (T6) also exist. On [12, p. 3], Kurz attributes to Menger [13] the

Lemma 2.7. *If $\sigma = (1, 2, 3)$, then*

$$\text{fix}(\sigma) = \begin{cases} 0 & \text{if } n \not\equiv 0 \pmod{3} \\ \lfloor \frac{n}{3+\sqrt{3}} \rfloor & \text{if } n \equiv 0 \pmod{3}. \end{cases}$$

Proof. As noted above, $\text{Fix}(\sigma)$ consists of the graphs from \mathcal{T}_n whose edge-labels (as in Figure 2) satisfy $A = B = C$ and $a = b = c$. Such a graph corresponds to a tetrahedron of the form shown in Figure 7 (left). If such a tetrahedron exists, then from $n = 3A + 3a$ we must have $n \equiv 0 \pmod{3}$, and $a = \frac{n}{3} - A$. Then we note that (T2) is trivial, while (T3) is equivalent to the assertion that there is an (A, a, a) -triangle; the latter is equivalent to $A < 2a$, and hence by integrality to $A + 1 \leq 2a = \frac{2n}{3} - 2A$. Keeping in mind that A is an integer, the latter gives

$$A \leq \left\lfloor \frac{2n-3}{9} \right\rfloor. \quad (2.8)$$

For (T6), we have $x_1 = x_2 = \frac{A}{2}$, $Y_1 = \frac{3A^2}{4}$ and $Y_2 = a^2 - \frac{A^2}{4}$, and the inequality in (T6) becomes $\frac{A^4}{4} < 3A^2(a^2 - \frac{A^2}{4})$. Rearranging, and remembering that $A, a > 0$, this gives $A < \sqrt{3}a = \sqrt{3}(\frac{n}{3} - A)$, and so $A < \frac{n}{3+\sqrt{3}}$. Since A is an integer, and since $\frac{n}{3+\sqrt{3}}$ is irrational, it follows that

$$A \leq \left\lfloor \frac{n}{3+\sqrt{3}} \right\rfloor. \quad (2.9)$$

One may show that $\frac{2n-3}{9} \geq \frac{n}{3+\sqrt{3}} \Leftrightarrow n \geq 31$, and also that $\lfloor \frac{2n-3}{9} \rfloor = \lfloor \frac{n}{3+\sqrt{3}} \rfloor$ if $n \leq 30$ is a multiple of 3. The result then follows from (2.8) and (2.9). \square

Lemma 2.10. *If $\sigma = (1, 2, 4, 3)$, then*

$$\text{fix}(\sigma) = \begin{cases} 0 & \text{if } n \not\equiv 0 \pmod{2} \\ \lfloor \frac{n}{4+4\sqrt{2}} \rfloor & \text{if } n \equiv 0 \pmod{4} \\ \lfloor \frac{n+2+2\sqrt{2}}{4+4\sqrt{2}} \rfloor & \text{if } n \equiv 2 \pmod{4}. \end{cases}$$

Proof. This time $\text{Fix}(\sigma)$ consists of the graphs from \mathcal{T}_n whose edge-labels (as in Figure 2) satisfy $A = a$ and $B = C = b = c$. Such a graph corresponds to a tetrahedron of the form shown in Figure 7 (right). If such a tetrahedron exists, then from $n = 2A + 4B$ we must have $n \equiv 0 \pmod{2}$, $A \equiv \frac{n}{2} \pmod{2}$ and $B = \frac{n-2A}{4}$. Then we note that (T2) and (T3) are both equivalent to $A < 2B$, and hence to $A + 1 \leq 2B = \frac{n}{2} - A$. The latter gives

$$A \leq \left\lfloor \frac{n-2}{4} \right\rfloor. \quad (2.11)$$

Rather than (T6), it is more convenient to work with the equivalent $|PQ|^2 < a^2 < |PR|^2$ from the proof of Proposition 2.5; cf. Figure 6. Since $P = Q$ (and remembering that $A = a$, etc.), this is equivalent to $A^2 < 4B^2 - A^2$, which gives $A < \sqrt{2}B = \frac{n-2A}{2\sqrt{2}}$, and ultimately

$$A \leq \left\lfloor \frac{n}{2+2\sqrt{2}} \right\rfloor. \quad (2.12)$$

This time, $\frac{n-2}{4} \geq \frac{n}{2+2\sqrt{2}} \Leftrightarrow n \geq 12$, and also $\lfloor \frac{n-2}{4} \rfloor = \lfloor \frac{n}{2+2\sqrt{2}} \rfloor$ if $n \leq 10$ is even. Thus, if we write $K = \lfloor \frac{n}{2+2\sqrt{2}} \rfloor$, then it follows from (2.11) and (2.12) that $\text{fix}(\sigma)$ is equal to the cardinality of the set

$$X = \{A \in \mathbb{N} : A \leq K, A \equiv \frac{n}{2} \pmod{2}\}.$$

Now,

$$|X| = \begin{cases} \lfloor \frac{K}{2} \rfloor & \text{if } \frac{n}{2} \equiv 0 \pmod{2}: \text{ i.e., if } n \equiv 0 \pmod{4} \\ \lfloor \frac{K+1}{2} \rfloor & \text{if } \frac{n}{2} \equiv 1 \pmod{2}: \text{ i.e., if } n \equiv 2 \pmod{4}. \end{cases}$$

The result then follows from the definition of K , and the fact that $\lfloor \frac{\lfloor x \rfloor}{2} \rfloor = \lfloor \frac{x}{2} \rfloor$ for real x . \square

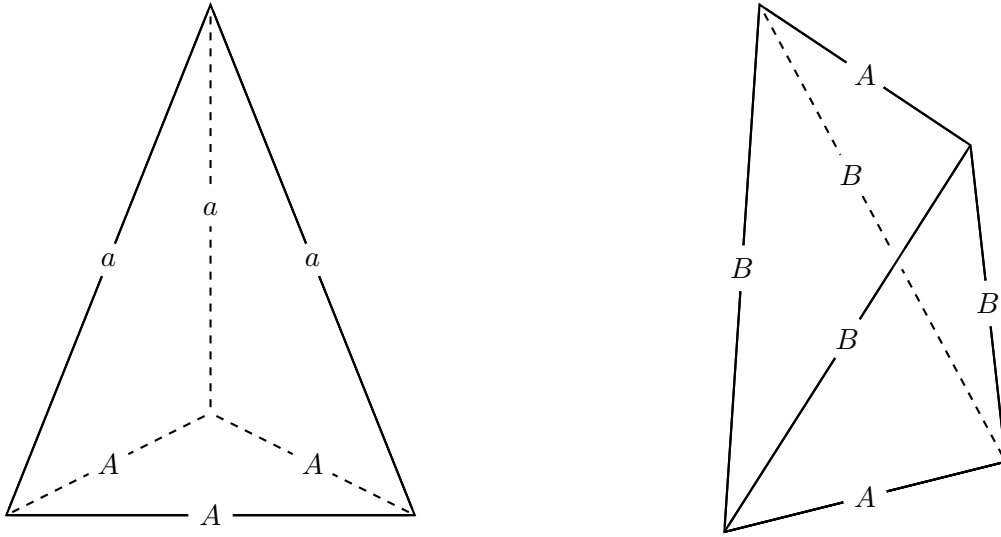


Figure 7. Tetrahedra from the proofs of Lemmas 2.7 and 2.10.

As noted above, we are currently unable to calculate $\text{fix}(\sigma)$ for σ of types (i), (iii) and (iv). It is possible that types (iii) and (iv) could be treated by more elaborate versions of the arguments given in Lemmas 2.7 and 2.10. Calculated values of all $\text{fix}(\sigma)$ parameters for $1 \leq n \leq 100$ are given in Table 5; see also Figures 17–19. If one could calculate $\text{fix}(\text{id}_4) = |\mathcal{T}_n|$, this would have important consequences for the asymptotics of t_n itself; see Section 4.1.

Remark 2.13. The arguments of this section can be modified to calculate the numbers ${}^d t$ or ${}^d t_n$. Consider the following condition on a graph G from \mathcal{G} , as shown in Figure 2 (centre):

$$(T1)' \max\{A, B, C, a, b, c\} = d.$$

Then the set ${}^d \mathcal{T}$ of graphs from \mathcal{G} corresponding to integer tetrahedra of diameter d are precisely those satisfying (T1)' and (T2)–(T6); cf. Proposition 2.5. The set ${}^d \mathcal{T}_n = \mathcal{T}_n \cap {}^d \mathcal{T}$ of graphs from \mathcal{G} corresponding to integer tetrahedra of perimeter n and diameter d are precisely those satisfying (T1)' and (T1)–(T6). Then

$${}^d t = |{}^d \mathcal{T} / \mathcal{S}_4| \quad \text{and} \quad {}^d t_n = |{}^d \mathcal{T}_n / \mathcal{S}_4|$$

are given by counting orbits of the action of \mathcal{S}_4 given in (2.1). We also have the numbers ${}^d t'$ and ${}^d t'_n$, counting tetrahedra (of relevant parameters) up to rotations only, and these are given in terms of the restricted action of \mathcal{A}_4 .

3 Computation and data

In the previous section we gave a method for (in principle) computing the numbers t_n , ${}^d t$ and ${}^d t_n$. Given that we are currently unable to give explicit formulas for the $\text{fix}(\sigma)$ parameters in certain cases, and hence for the t_n , ${}^d t$ and ${}^d t_n$ sequences themselves, we now turn to some computations to make further progress. In this section we discuss algorithms/code, and give several tables and graphs of calculated values. In the next section we make some observations and conjectures based on the computational data.

3.1 Enumeration algorithms

To compute or enumerate all tetrahedra of a given perimeter n , we identify the graph G from Figure 2 with the 6-tuple $[(A, a), (B, b), (C, c)]$. This is clearly a tuple over $\{1, \dots, n\}$, though we will see in Lemma 3.2 that the entries of the tuple belong to a much smaller range; at this point, it is obvious at

least that no entry could be bigger than $n - 5$. The orbits of G (as in Figure 2) under the action of \mathcal{S}_4 given in (2.1) correspond to the following tuples:

$$\begin{aligned}
& [(A, a), (B, b), (C, c)], & [(A, a), (b, B), (c, C)], & [(a, A), (B, b), (c, C)], & [(a, A), (b, B), (C, c)], \\
& [(C, c), (A, a), (B, b)], & [(c, C), (A, a), (b, B)], & [(c, C), (a, A), (B, b)], & [(C, c), (a, A), (b, B)], \\
& [(B, b), (C, c), (A, a)], & [(b, B), (c, C), (A, a)], & [(B, b), (c, C), (a, A)], & [(b, B), (C, c), (a, A)], \\
& [(A, a), (C, c), (B, b)], & [(A, a), (c, C), (b, B)], & [(a, A), (c, C), (B, b)], & [(a, A), (C, c), (b, B)], \\
& [(B, b), (A, a), (C, c)], & [(b, B), (A, a), (c, C)], & [(B, b), (a, A), (c, C)], & [(b, B), (a, A), (C, c)], \\
& [(C, c), (B, b), (A, a)], & [(c, C), (b, B), (A, a)], & [(c, C), (B, b), (a, A)], & [(C, c), (b, B), (a, A)].
\end{aligned} \tag{3.1}$$

Each of these can be alternatively obtained from $[(A, a), (B, b), (C, c)]$ by the action of a signed permutation τ of the set $\{1, 2, 3\}$. Roughly speaking, the non-signed part of τ tells us how to move the pairs (A, a) , (B, b) and (C, c) , and the signed part tells us whether (X, x) is listed in the final arrangement as (X, x) or is flipped to (x, X) . Moreover, examining (3.1), only those signed permutations with an even number of flips occur. This means that we are dealing with an action of the Coxeter group of type D_3 , which is well-known to be isomorphic to the symmetric group \mathcal{S}_4 (type A_3). For more on Coxeter groups, see [9].

The most obvious algorithm for creating the set \mathcal{T}_n would be to take all 6-tuples $[(A, a), (B, b), (C, c)]$ over $\{1, \dots, n - 5\}$, and keep those satisfying conditions (T1)–(T6) from Proposition 2.5. Once we have the set \mathcal{T}_n , we can quickly compute the tuples fixed under the action of permutations σ from \mathcal{S}_4 of types (i)–(v), and thereby compute $t_n = \frac{1}{24} \sum_{\sigma} \text{fix}(\sigma)$.

On the other hand, since we are ultimately concerned with counting *orbits*, we do not need to store *all* tuples from \mathcal{T}_n ; we only need to store a single representative: e.g., the lex-greatest such tuple.

Some simple geometrical considerations allow us to reduce the search space, and also lead to other shortcuts.

Lemma 3.2. *If an integer tetrahedron has perimeter n and diameter d , then*

$$\left\lfloor \frac{n}{6} \right\rfloor \leq d \leq \left\lfloor \frac{n-3}{3} \right\rfloor \quad \text{or equivalently} \quad 3d + 3 \leq n \leq 6d.$$

Proof. It suffices to prove the second system of inequalities, and we note that $n \leq 6d$ is clear.

Consider the graph G pictured in Figure 2, and assume by symmetry that $d = A$. From the (A, B, C) - and (A, b, c) -triangles we obtain $B + C \geq A + 1$ and $b + c \geq A + 1$, and so

$$n = A + (B + C) + a + (b + c) \geq A + (A + 1) + 1 + (A + 1) = 3d + 3. \quad \square$$

Remark 3.3. For fixed d , the maximum value of $n = 6d$ occurs uniquely, of course, for the equilateral tetrahedron $[(d, d), (d, d), (d, d)]$. The minimum value of $n = 3d + 3$ corresponds to $[(1, d), (1, d), (1, d)]$, for example, a very “thin” tetrahedron of the form shown in Figure 7 (left). In general, other tetrahedra have $n = 3d + 3$: e.g., $[(1, d), (2, d - 1), (2, d - 1)]$ for $d \geq 3$.

Remark 3.4. Although every edge of an integer tetrahedron of perimeter n is bounded above by $\lfloor \frac{n-3}{3} \rfloor$, it is not true that $\lceil \frac{n}{6} \rceil$ is a lower bound for all edges. Indeed, we have the very “thin” tetrahedra $[(1, d), (1, d), (1, d)]$ and $[(d, d), (d, d), (1, 1)]$, as in Figure 7.

Similar considerations apply to the triangular faces:

Lemma 3.5. *If an integer tetrahedron has perimeter n and maximum face-perimeter M , then*

$$\left\lfloor \frac{n}{2} \right\rfloor \leq M \leq \left\lfloor \frac{2n-3}{3} \right\rfloor \quad \text{or equivalently} \quad \left\lceil \frac{3M+3}{2} \right\rceil \leq n \leq 2M.$$

Proof. It suffices to show that $\frac{3M+3}{2} \leq n \leq 2M$. To do so, consider the graph G pictured in Figure 2, assuming by symmetry that $M = A + B + C$. Adding the perimeters of all four faces gives twice the

perimeter of the tetrahedron. The first consequence of this is that $2n \leq 4M$: i.e., $n \leq 2M$. The second consequence (also using $b + c \geq A + 1$, etc., from the other triangular faces) is that

$$\begin{aligned} 2n &= (A + B + C) + (A + b + c) + (B + a + c) + (C + a + b) \\ &\geq (A + B + C) + (A + A + 1) + (B + B + 1) + (C + C + 1) = 3(A + B + C) + 3 = 3M + 3, \end{aligned}$$

which gives $n \geq \frac{3M+3}{3}$. □

With the above considerations in mind, a simple algorithm for calculating a set of representatives of ${}^d\mathcal{T}_n$ is as follows. Here we write $d = A$ to keep the notation as in Figure 2. Roughly speaking, we create tetrahedra as in Figure 6, with the diameter on the x -axis.

- (I) Define the set $S = \emptyset$.
- (II) Create the set of all triangles with maximum side $A (= d)$ and with perimeter at most $\lfloor \frac{2n-3}{3} \rfloor$. (This is fairly routine, so the details are omitted.)
- (III) Then for each pair (A, B, C) and (A, b, c) of such triangles, we set $a = n - (A + B + C + b + c)$.
- (IV) If $a \leq A$ and if the tuple $T = [(A, a), (B, b), (C, c)]$ satisfies condition (T6) from Proposition 2.5, we add to the set S the lex-greatest representative of T from the list (3.1).

The number ${}^d t_n = A t_n$ is then the size of the set S created. Summing over all d (or n) gives t_n (or ${}^d t$), respectively. There are many easy ways to simplify the above. For example, the sixth entry of the tuple $[(A, a), (B, b), (C, c)]$ does not need to be stored, as it can be inferred from the others; neither do we need to store the first entry as this is always d (this is why we chose to store the lex-greatest representative).

We carried out the above algorithm in a variety of languages. We were able to calculate t_n up to $n = 1100$ before running out of memory on standard laptops (even for single values of d). It was around this stage in our investigations that we discovered Kurz’s article [12]. We regret to say that the “integral” rather than “integer” in his title defeated our searching abilities. Additionally, since we were initially interested only in the t_n sequence, we initially found only Sequence A208454 on the OEIS [1], but not A097125, which contains many terms in the ${}^d t$ sequence.

The most significant advantage of Kurz’s algorithm for enumeration by diameter is that it does not require the creation and storage of vast numbers of tuples. Rather, it moves through “tuple space” in such an orderly fashion that each canonical tuple is visited once, meaning that these only have to be counted rather than stored. Our current algorithms are modifications of Kurz’s, implemented in C, and with a number of optimisations, including parallelisation and use of the GNU Multiple Precision Arithmetic Library to store and manipulate large integers. All of our calculations of the numbers ${}^d t$ match those given by Kurz, though we have gone somewhat further; see Table 8.

3.2 Values

So far we have calculated t_n for every $1 \leq n \leq 3000$, and for several other values up to $n = 20000$. Various tables and figures in this section summarise some of these calculations, but more complete lists are available at [3]. Some of the tables below also include values of ${}^d t$, ${}^d t_n$ and t'_n (tetrahedra up to rotations and translations only), and also $\text{fix}(\sigma)$ for certain permutations $\sigma \in \mathcal{S}_4$. (More extensive tables containing values of ${}^d t$ are given by Kurz [12].) For convenience of reference, here is a summary of the content of the tables and figures given in this section (more are given in Section 4, and we note that some of the tables in the current section also include additional parameters defined in Section 4):

Location	Numbers	Range	Comments	
Table 1	t_n	$1 \leq n \leq 200$	by hundreds	
Table 2	t_n	$1 \leq n \leq 10000$		
Table 3	$d_t t_n$	$1 \leq n \leq 50$		
Table 4	$d_t t_n$	$1 \leq n \leq 200$		
Table 5	$\text{fix}(\sigma), t_n, t'_n$	$1 \leq n \leq 100$		
Table 7	t_n	$1 \leq n \leq 20000$		by thousands
Table 8	d_t	$1 \leq d \leq 2000$		by hundreds
Figure 8	t_n	$1 \leq n \leq 30$		log-log plot by hundreds heat map and discrete derivative and discrete derivative $\sigma \in \mathcal{S}_4$
Figure 9	t_n	$1 \leq n \leq 200$		
Figure 10	t_n	$1 \leq n \leq 200$		
Figure 11	t_n	$1 \leq n \leq 10000$		
Figure 12	$d_t t_n$	$1 \leq n \leq 2000$		
Figure 13	$d_t t_n$	$n = 100$ and 200		
Figure 14	$d_t t_n$	$n = 10000$		
Figure 15	$d_t t_n$	$d = 50$ and 100		
Figure 16	$d_t t_n$	$d = 1000$		
Figures 17–19	$\text{fix}(\sigma)$	$1 \leq n \leq 100$		

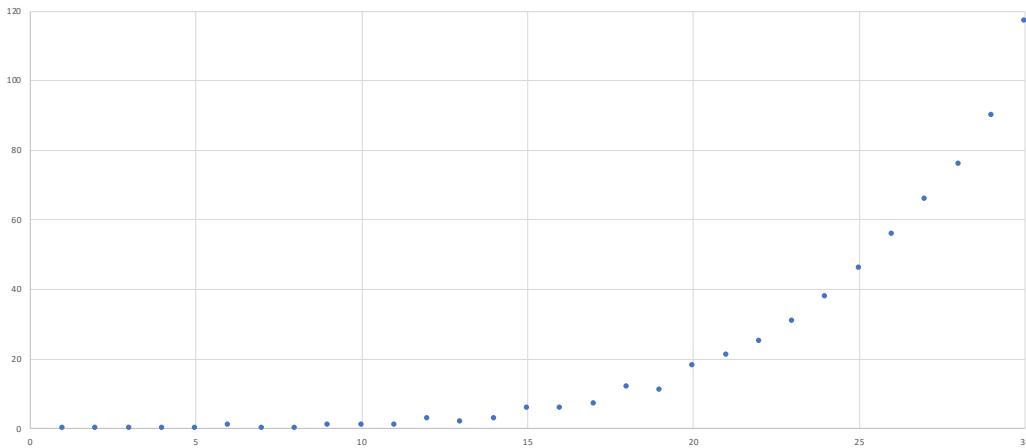


Figure 8. Calculated values of t_n , $1 \leq n \leq 30$.

4 Observations from the data

The computational data presented in Section 3 has allowed us to discover some interesting patterns, and has led to a number of natural conjectures, which we discuss in the current section. We do not mean to imply that the following discussion is exhaustive. We hope that other researchers may be able to shed light on some of our conjectures, and make further discoveries.

4.1 Asymptotics

First and foremost, we had hoped that the computed values of t_n might have suggested an obvious formula, perhaps after consultation with the OEIS [1]. However, this regrettably was not the case. The “bumpy” nature of the t_n sequence, which can be seen in Figure 8, suggests there is no simple formula. However, the sequence does appear to become smoother at a larger scale, as can be seen in

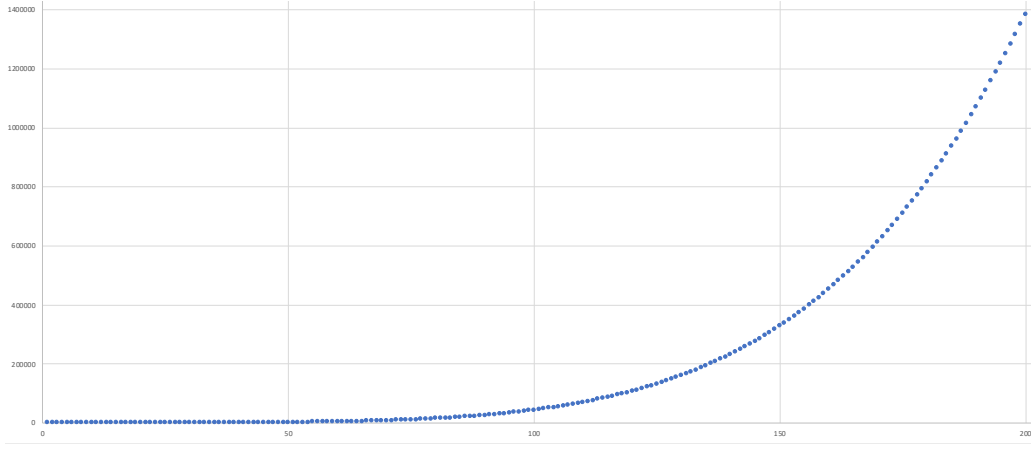


Figure 9. Calculated values of t_n , $1 \leq n \leq 200$.

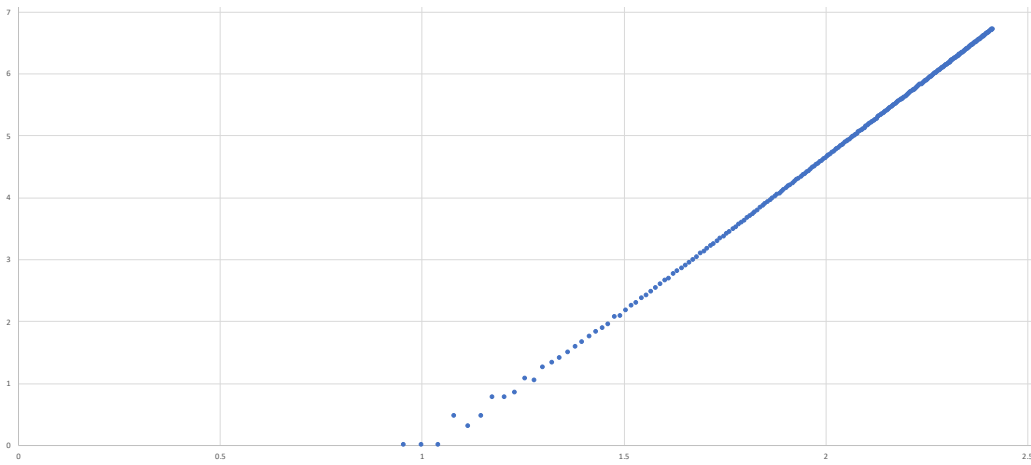


Figure 10. Log-log plot of calculated values of t_n , $1 \leq n \leq 200$.

Figure 9. This is (apparently) confirmed further in Figure 10, which gives a log-log plot, and suggests a possible power law.

By analogy with the case of triangles, where the answer is asymptotic to $\frac{n^2}{48}$ (cf. Honsberger's Theorem), we might wonder if $t_n \sim \frac{n^k}{C}$ for some integers k and C . If this were so, then

$$\frac{t_{n+1}}{t_n} \sim \frac{(n+1)^k}{n^k} = \frac{n^k + kn^{k-1} + \dots}{n^k} \sim 1 + \frac{k}{n}.$$

Computed values of $\left(\frac{t_{n+1}}{t_n} - 1\right) \times n$ strongly suggest a likely value of $k = 5$. Computed values of $C_n = \frac{n^5}{t_n}$ suggest a possible value in the order of $C \approx 229000$. Table 6 gives calculated values of C_n for n up to 10000 (by hundreds); Table 7 goes up to $n = 20000$ (by thousands). The third column of Table 6 gives the difference $d_n = C_n - C_{n-100}$, which shows that the fall of C_n becomes slower as n increases. The values d_n are themselves decreasing, as governed by the ratio $r_n = d_n/d_{n-100}$. This ratio seems to be tending towards 0.98 or 0.99, or thereabouts. If so, then continuing the trend, C_n seems to approach 229028 or 229024, respectively. So we have the following tentative conjecture; we have made an explicit choice for the denominator so as to have a concrete statement, but there is some level of uncertainty, as just discussed.

Conjecture 4.1. *The number t_n of integer tetrahedra of perimeter n , up to congruence, satisfies*

$$t_n \sim \frac{n^5}{229024} \quad \text{as } n \rightarrow \infty.$$

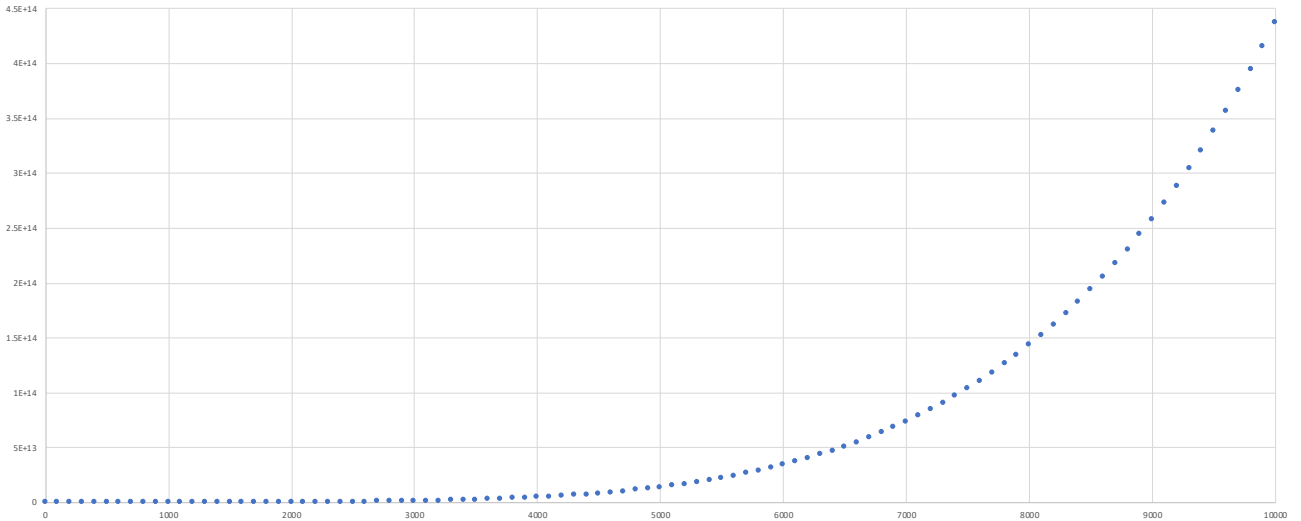


Figure 11. Calculated values of t_n , $1 \leq n \leq 10000$ (by hundreds).

Taking Conjecture 4.1 as given, one could then aim to analyse the sequence $s_n = t_n - \frac{n^5}{229024}$. For example, one might hope that this is a quartic polynomial. As above, evidence for this could be gathered by calculating values of $\left(\frac{s_{n+1}}{s_n} - 1\right) \times n$. However, these values appear to be quite chaotic, even when we look at different values of C around the conjectured value of 229024. However, we have more success by splitting up the s_n sequence, and looking at subsequences $s_i, s_{i+k}, s_{i+2k}, \dots$, for various integers $k \geq 2$ and for each $0 \leq i \leq k-1$, especially when k is a multiple of 12. Here the relevant value to calculate is $\left(\frac{s_{n+k}}{s_n} - 1\right) \times \frac{n}{k}$, and this does seem to approach 4 as $n \rightarrow \infty$ (for $k \equiv 0 \pmod{12}$), for various C . Might there be a multi-case formula for t_n ? Attempts to fit polynomials to subsequences (of the kind described above), using various statistical packages, have not led to any success. In any case, the uncertainty as to the value of $C \approx 229024$ leads to even greater uncertainty here.

Here is an additional note about Conjecture 4.1 (we will return to it again in Section 4.5). Recall that $t_n = \frac{1}{24} \sum_{\sigma \in \mathcal{S}_4} \text{fix}(\sigma)$; cf. (2.2). For $\sigma \in \mathcal{S}_4 \setminus \{\text{id}_4\}$, it is easy to see that $\text{fix}(\sigma)$ is bounded above by n^4 ; this can be seen by examining the constraints on the labels of a graph G fixed by σ in cases (ii)–(v), as listed in Section 2. Thus, if t_n is indeed (asymptotically) a quintic, then so too is $\text{fix}(\text{id}_4) = |\mathcal{T}_n|$, and so

$$t_n \sim \frac{|\mathcal{T}_n|}{24} \quad \text{as } n \rightarrow \infty.$$

This can be interpreted as saying that virtually all tetrahedra have no symmetry at all. It also leads to an equivalent formulation of Conjecture 4.1, again subject to some uncertainty in the value of the stated numerical coefficient:

Conjecture 4.2. *The set \mathcal{T}_n of graphs corresponding to integer tetrahedra of perimeter n satisfies*

$$|\mathcal{T}_n| \sim \frac{3n^5}{28628} \quad \text{as } n \rightarrow \infty.$$

Remark 4.3. Asymptotics of the numbers ${}^d t$ were not discussed explicitly by Kurz [12]. However, it was observed on [12, p. 7] that ${}^d t$ seems to be approximately 0.103 times the number of graphs from \mathcal{G} satisfying (T1)' and (T2)–(T5); see Proposition 2.5 and Remark 2.13. The language used in [12] was different, and instead spoke of symmetric matrices, but it follows from [12, Lemma 4] that the number of such graphs/matrices is asymptotic to $\frac{d^5}{4}$. Thus, a tentative conjecture for an asymptotic expression for ${}^d t$ is

$${}^d t \sim 0.103 \times \frac{d^5}{4} \approx \frac{d^5}{38.835} \quad \text{as } d \rightarrow \infty. \quad (4.4)$$

This fares quite well with computed values; see Table 8. The non-integrality of the denominator 38.835 in (4.4) suggests that the denominator in Conjecture 4.1 for the t_n sequence might not be an integer either. Again, we will say more about this in Section 4.5.

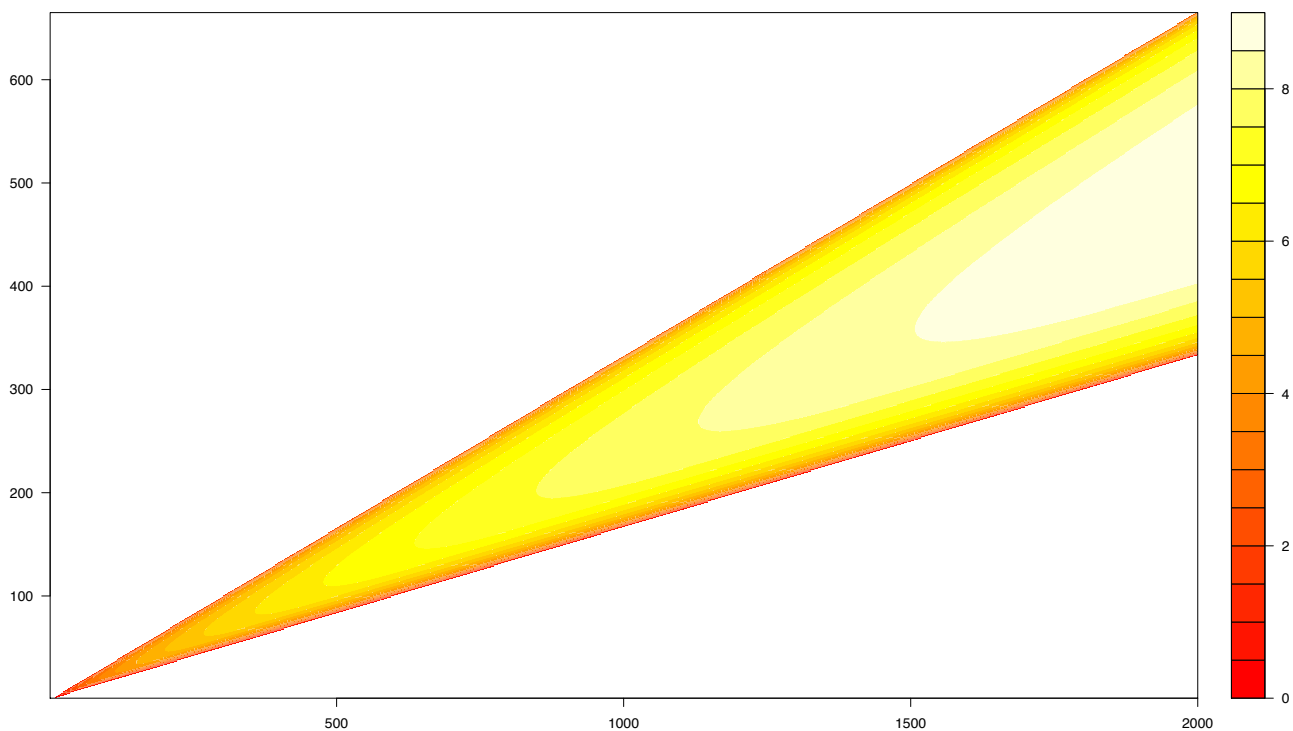


Figure 12. Heat map of the numbers $\log_{10}(^d t_n)$, with $1 \leq n \leq 2000$ and $1 \leq d \leq 666$ on the horizontal and vertical axes, respectively.

4.2 Distributions

Looking at Figures 13 and 14, which graph the numbers $^d t_{100}$, $^d t_{200}$ and $^d t_{10000}$ (for all allowable values of d), one sees a general shape emerging. In fact, by plotting scaled graphs of $^d t_n$, one sees that the shapes are essentially identical, up to scale; several such graphs can be seen at [3], including some animations. This means that in principle one might be able to estimate the value of (say) t_{30000} by interpolating the shape of the $^d t_{30000}$ curve from the $^d t_{10000}$ or $^d t_{20000}$ curve (for which we have full data), and calculating a few of the maximum values of $^d t_{30000}$ to obtain the scaling factor. Table 7 gives the maximum values of $^d t_{30000}$ and $^d t_{40000}$, which occur at $d = 7140$ and $d = 9520$, respectively. The maximum value of $^d t_n$ seems to regularly occur when $d \approx 0.238n \approx \frac{n}{4.2}$. We do not currently know the significance of this number. We will come back to this point in Section 4.5.

Since there are so many points, Figure 14 appears to show a number of continuous curves. The dark blue “curve” plots the sequence $^d t_{10000}$ ($1667 \leq d \leq 3332$), while the orange “curve” is the discrete derivative of this sequence: i.e., the values of $^d t_{10000} - {}^{d-1} t_{10000}$. (The meaning of the light blue curve will be explained in Section 4.4.) Thus, the orange curve is (an approximation to) the derivative of the blue curve. One may see that although the orange curve appears to be continuous, there is a sharp corner just after the maximum slope (which occurs at around $d = 2073$).

Similarly, Figures 15 and 16 graph the numbers $^{50} t_n$, $^{100} t_n$ and $^{1000} t_n$ (for all allowable values of n), and again one sees a general shape emerging. Again Figure 16 shows the discrete derivative of the $^{1000} t_n$ sequence (in orange); although it is not as easy to see, the orange curve also has a sharp corner, this time just before the minimum slope (which occurs at around $n \approx 4830$).

The data used to create Figure 16 also allows one to calculate

$${}^{1000} t = \sum_{n=3003}^{6000} {}^{1000} t_n = 25728695195597,$$

which agrees with the largest computed value given by Kurz in [12, Table 2]. Some further values of $^d t$ (up to $d = 2000$) are given in Table 8.

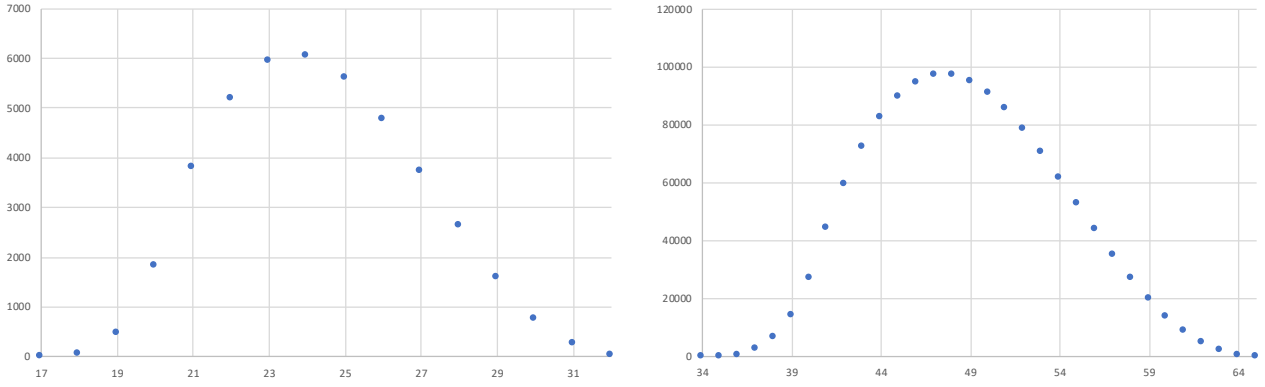


Figure 13. Calculated values of $d_{t_{100}}$ (left) and $d_{t_{200}}$ (right).

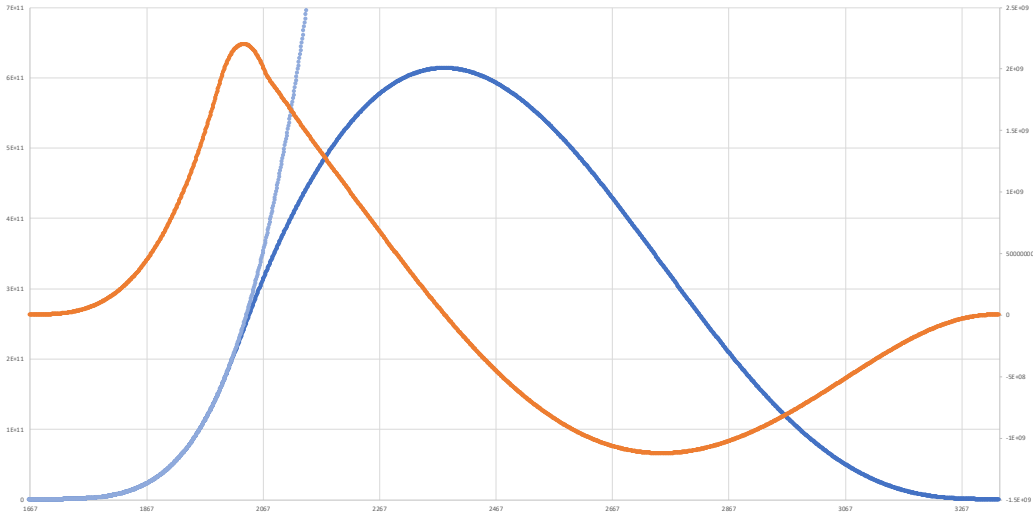


Figure 14. Calculated values of $d_{t_{10000}}$ (dark blue) and the discrete derivative (orange). The light blue curve is explained in Section 4.4.

4.3 Scratching the surface: maximal diameter

Tables 3 and 4 give values of d_{t_n} , and a couple of simple patterns seem to emerge when looking at the right-most entry of each row, corresponding to the maximum d for a fixed n . Specifically, we see the three sequences

$$1, 1, 2, 2, 3, 3, \dots, \quad 0, 1, 2, 3, 4, 5, \dots, \quad 0, 1, 3, 6, 10, 13, 16, 19, 22, 25, 28, 31, 34, \dots, \quad (4.5)$$

corresponding to $n \equiv 0$, $n \equiv 1$ and $n \equiv 2 \pmod{3}$, respectively. These are the numbers

$$d_{t_{3d+3}} \ (d = 1, 2, 3, \dots), \quad d_{t_{3d+4}} \ (d = 1, 2, 3, \dots), \quad d_{t_{3d+5}} \ (d = 1, 2, 3, \dots),$$

respectively. The apparent patterns in the first two sequences are obvious; it appears that

$$d_{t_{3d+3}} = \lceil \frac{d}{2} \rceil \quad \text{and} \quad d_{t_{3d+4}} = d - 1 \quad \text{for } d \geq 1.$$

There are simple explanations for these. We give the details for the first, and sketch them for the second. (We will consider the third sequence later.) We begin with a simple observation:

Lemma 4.6. *Any altitude of an integer triangle is greater than $1/\sqrt{2}$.*

Proof. Let the side-lengths of the triangle be $a \leq b \leq d$, and let x be any of a, b, d . Let h be the altitude measured from a side of length x , and denote the area of the triangle by $A = xh/2$. By Heron's

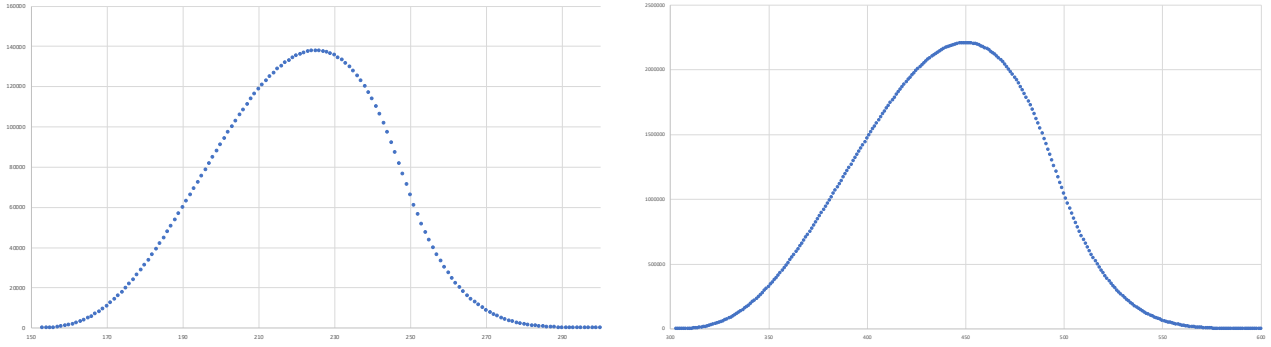


Figure 15. Calculated values of ${}^{50}t_n$ (left) and ${}^{100}t_n$ (right).

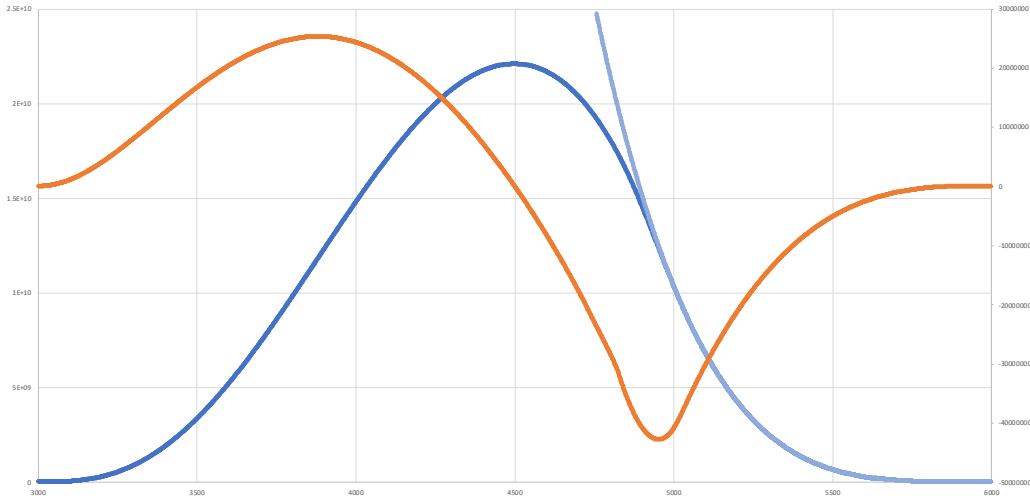


Figure 16. Calculated values of ${}^{1000}t_n$ (dark blue) and the discrete derivative (orange). The light blue curve is explained in Section 4.4.

formula, and keeping $a \leq b \leq d$ and $a + b \geq d + 1$ in mind, we have

$$\begin{aligned} h^2 &= \frac{4A^2}{x^2} \geq \frac{4A^2}{d^2} = \frac{4}{d^2} \cdot \frac{1}{16} \cdot (a + b + d) \cdot (a + b - d) \cdot (a - b + d) \cdot (-a + b + d) \\ &\geq \frac{1}{4d^2} \cdot (2d + 1) \cdot 1 \cdot a \cdot d > \frac{2ad^2}{4d^2} = \frac{a}{2} \geq \frac{1}{2}. \end{aligned}$$

The result follows. □

Remark 4.7. If the shortest side of an integer triangle is at least 2, then it follows from the above proof that any altitude is greater than 1. Of course this is not true if the shortest side has length 1, and if the altitude is measured from one of the two sides of length d ; in fact it is easy to show that $h^2 = 1 - 1/4d^2$ in this case. Since the latter is decreasing in d , and equal to $3/4$ when $d = 1$, the lower bound of $1/\sqrt{2} \approx 0.707$ in Lemma 4.6 could be replaced by $\sqrt{3}/2 \approx 0.866$, though the latter is not a *strict* lower bound.

Lemma 4.8. *For any $d \geq 1$ we have ${}^d t_{3d+3} = \lceil \frac{d}{2} \rceil$.*

Proof. First consider an integer triangle with side-lengths $B \leq C \leq d$ satisfying $B + C = d + 1$, and join two copies of this triangle together in the way shown in Figure 20. By Lemma 4.6, we can fold these towards each other (as in Figure 6) until the tips are 1 unit apart, thus obtaining an integer tetrahedron of diameter d and perimeter $3d + 3$. There are $\lceil \frac{d}{2} \rceil$ such triangles, and they give rise to pairwise-noncongruent tetrahedra.

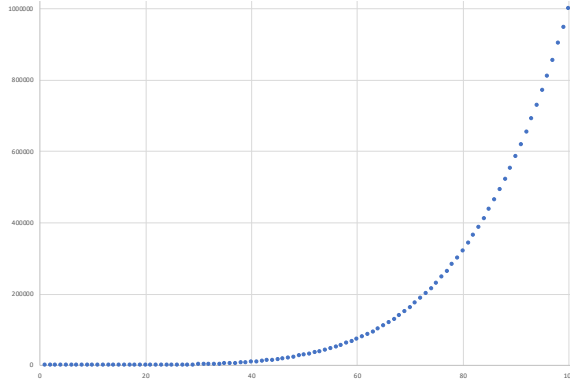


Figure 17. Calculated values of $\text{fix}(\sigma)$, for σ of type (i), $1 \leq n \leq 100$.

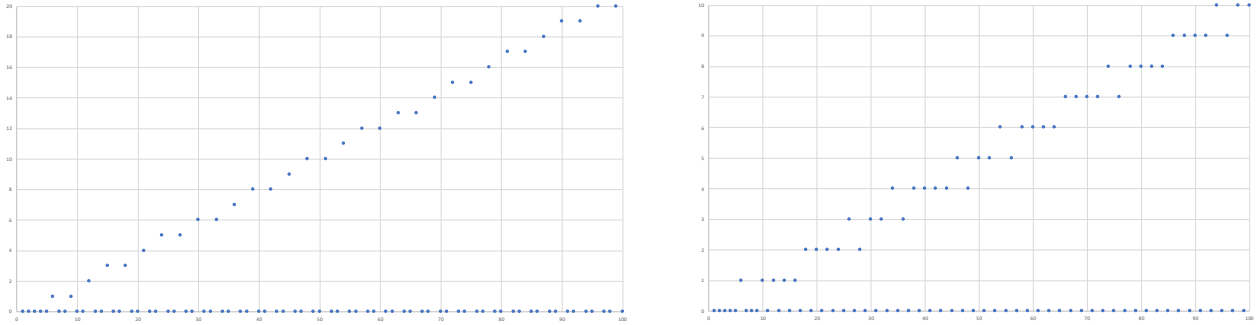


Figure 18. Left and right: calculated values of $\text{fix}(\sigma)$, for σ of type (ii) and (v), $1 \leq n \leq 100$; cf. Lemmas 2.7 and 2.10.

Conversely, let T be an arbitrary tetrahedron with diameter d and perimeter $n = 3d + 3$. We can construct T by folding, as in Figure 6, assuming that $A = d$ and $B \leq C$. To ensure that $n = 3d + 3$ we must of course have $B + C = b + c = d + 1$ and $a = 1$. To complete the proof, we must show that $B = c$, as then also $C = b$. Aiming for a contradiction, suppose instead that $B \neq c$, and consider the points P and Q as shown in Figure 6. These are on the circles $x^2 + y^2 = B^2$ and $x^2 + y^2 = c^2$, respectively. Since B and c differ by at least 1 (as they are distinct positive integers), it follows that $|PQ| \geq 1 = a$. But this contradicts $|PQ| < a < |PR|$ from the proof of Proposition 2.5. \square

Lemma 4.9. *For any $d \geq 1$ we have $d_{t_{3d+4}} = d - 1$.*

Sketch of proof. Again we must analyse the pairs of triangles (B, C, d) and (b, c, d) that can be folded to create appropriate tetrahedra, as in Figure 6 (with $A = d$). Up to symmetry, this time we have either

- (a) $B + C = b + c = d + 1$ and $a = 2$, or else
- (b) $B + C = d + 1$, $b + c = d + 2$ and $a = 1$.

We first note that case (b) never actually occurs. Indeed, here, since $B + C \neq b + c$, we must either have $B \neq c$ or $C \neq b$ (or both). Considering circles, as in the proof of Lemma 4.8, we see that $|PQ| \geq 1 = a$, so the folding procedure cannot be carried out.

This leaves us to consider case (a), and we assume without loss of generality that $B \leq c$. Again considering circles, B and c cannot differ by more than 1, so we must have either

- (a1) $c = B$ (and $b = C$), or else
- (a2) $c = B + 1$ (and $b = C - 1$).

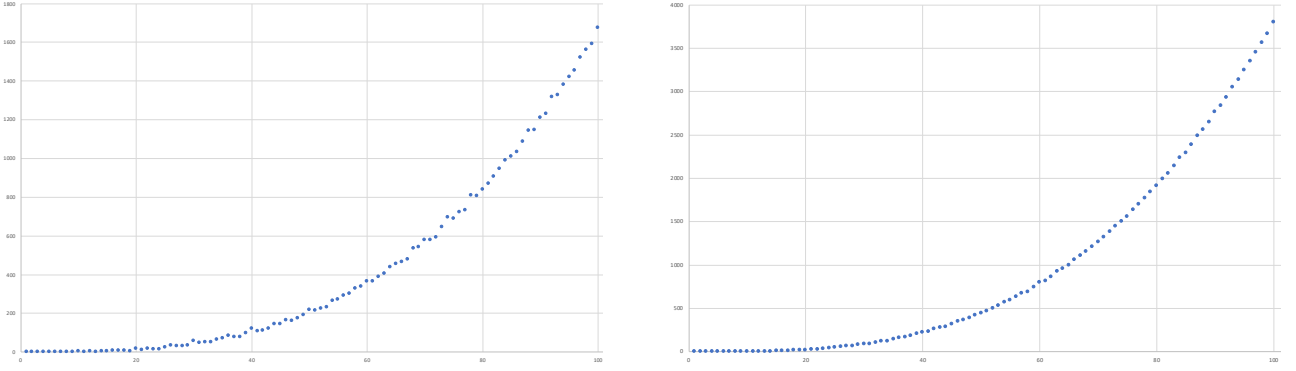


Figure 19. Left and right: calculated values of $\text{fix}(\sigma)$, for σ of type (iii) and (iv), $1 \leq n \leq 100$.

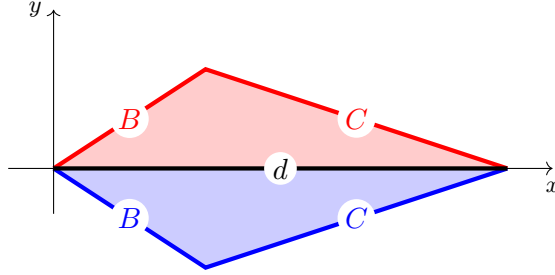


Figure 20. Creating an integer tetrahedron of diameter d and perimeter $n = 3d + 3$ by folding congruent triangles (with $B + C = d + 1$); see the proof of Lemma 4.8 for more details, and cf. Figure 6.

We consider these in turn, and show that there are $\lceil \frac{d}{2} \rceil - 1$ and $\lfloor \frac{d}{2} \rfloor$ tetrahedra in each case. Since these sum to $d - 1$, this will complete the proof.

(a1). By symmetry, we may also assume that $B \leq C (= d + 1 - B)$. So $1 \leq B \leq \lceil \frac{d}{2} \rceil$. Using Remark 4.7, we see that the folding procedure can be carried out in every case except for $B = 1$.

(a2). We again have $1 \leq B \leq \lceil \frac{d}{2} \rceil$, and this time the folding procedure can be carried out in each case. However, when d is odd, the $B = \lceil \frac{d}{2} \rceil - 1$ and $B = \lceil \frac{d}{2} \rceil$ cases produce congruent tetrahedra. So we obtain $\frac{d}{2}$ tetrahedra when d is even, and $\lceil \frac{d}{2} \rceil - 1$ when d is odd. In both cases, this is equal to $\lfloor \frac{d}{2} \rfloor$. \square

The behaviour of the third sequence in (4.5) appears to be rather more complex. For convenience in the following discussion, we will write $u_d = {}^d t_{3d+5}$ for $d \geq 1$. While these numbers seem to quickly stabilise into an arithmetic progression, $u_d = 3d - 5$ ($d \geq 5$), this only persists until $d = 41$, where we see an interesting change in the sequence:

..., 100, 103, 106, 109, 112, 115, 118, 115, 115, 116, 117, 118, 119, 121, 122, 124, 126, 127, 129, ...

The colours in the above lists are reflected in Tables 3 and 4, and we note that $u_{41} = 118$ and $u_{42} = 115$. The sequence of differences $u_{d+1} - u_d$ ($d \geq 42$) begins

0, 1, 1, 1, 1, 2, 1, 2, 2, 1, 2, 2, 1, 2, 2, 2, 1, 2, 2, 2, 2, 2, 2, 1, 2, 2, 2, 2, 2, 2, 2, 2, 1, ...

Although this appears somewhat chaotic, further calculations show that the last difference of 1 seems to occur at $d = 1110$, with all subsequent differences being 2. See Figure 21, which plots the differences $u_{d+1} - u_d$ (right), and also the ratios u_d/d (left). The above discussion suggests the possible formula

$$u_d = {}^d t_{3d+5} = 2d + 15 \quad \text{for } d \geq 1111. \quad (4.10)$$

We have verified this computationally up to $d = 50,000,000$. Interestingly, we obtained much better performance using the “naïve” algorithm described in Section 3.1 (see steps (I)–(IV)), as compared to

our modification of Kurz’s algorithm from [12]. (For example, the latter calculated $u_{3000} = 6015$ in around 2 hours, while the former took a fraction of a second; it calculated the 50,000,000th term in around 80 minutes.) The reason for this appears to be that our original algorithm directly creates and stores all tetrahedra with given dimensions, and then counts them; this led to serious memory issues in general, but for parameters n, d for which ${}^d t_n$ is relatively small (such as $n = 3d + 5$) this is actually an advantage. As discussed in Section 3.1, the Kurz-based algorithm moves through tuple space, counting or rejecting tuples as appropriate; it seems that when n is small relative to d , many more tuples are rejected than counted, leading to longer running times.

We have not attempted to prove (4.10), but we expect this could be done (if it is true) in a similar way to Lemmas 4.8 and 4.9 above. Computations suggest that for $d \geq 1111$, there are:

- $\lfloor \frac{d}{2} \rfloor - 1$ tetrahedra with $a = 1$,
- $\lceil \frac{3d}{2} \rceil - 3$ tetrahedra with $a = 3$, and
- 19 “sporadic” tetrahedra with $a = 2$,

and these sum to $2d + 15$. For smaller d the number of sporadic tetrahedra is different; for example, it is 20 for $205 \leq d \leq 1110$. Figure 22 plots the number of such sporadic tetrahedra for $1 \leq d \leq 2000$.

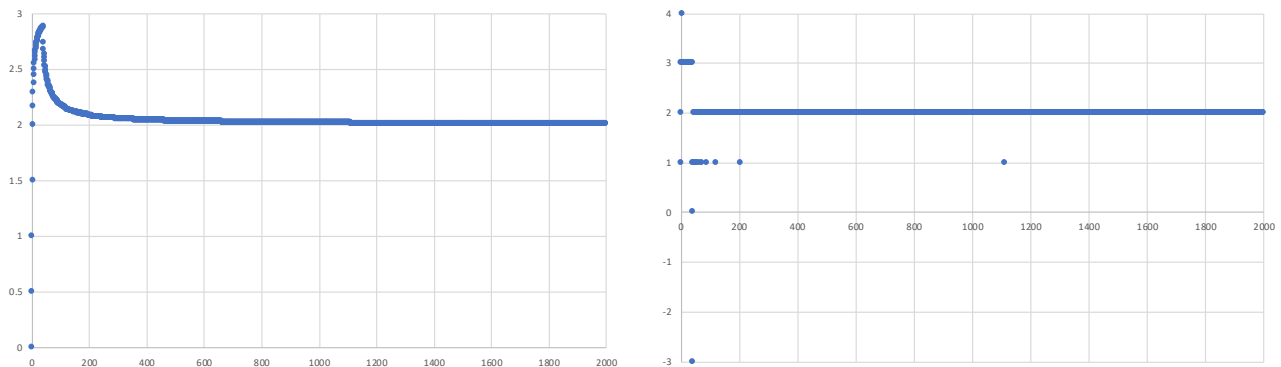


Figure 21. Left and right: calculated values of u_d/d and $u_{d+1} - u_d$, $1 \leq d \leq 2000$, where $u_d = {}^d t_{3d+5}$.

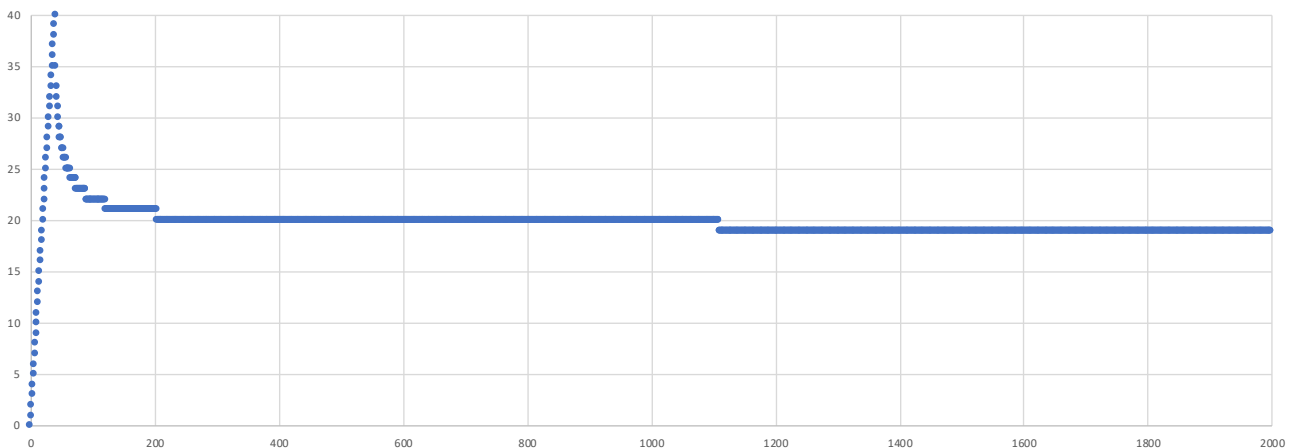


Figure 22. The number of “sporadic” tetrahedra with diameter d and perimeter $3d + 5$, $1 \leq d \leq 2000$; see Section 4.3 for more details.

We have not attempted to systematically study the numbers ${}^d t_{3d+k}$ for (fixed) $k \geq 6$, but Figure 23 gives some graphs of computed values for $k = 3, 4, \dots, 10$. It appears that for fixed k , the sequence ${}^d t_{3d+k}$ ($d = 1, 2, 3, \dots$) is eventually linear in d , but the “pre-linear” behaviour becomes more complex, and lasts longer as k increases. Taking $k = 10$, for example, and writing $v_d = {}^d t_{3d+10}$, Figure 24 shows the ratios v_d/d and differences $v_{d+1} - v_d$ (cf. Figure 21, which does the same for $k = 5$).

Both appear to approach a limit of 10, strongly suggesting that eventually $v_d = 10d + l$ for some l . Calculations suggest that $l = 2470$; this value of l holds for $2,000,000 \leq d \leq 20,000,000$. But we note that $l = 2471$ for $d = 1,000,000$, so that the “pre-linear” behaviour persists beyond the 1,000,000th term.

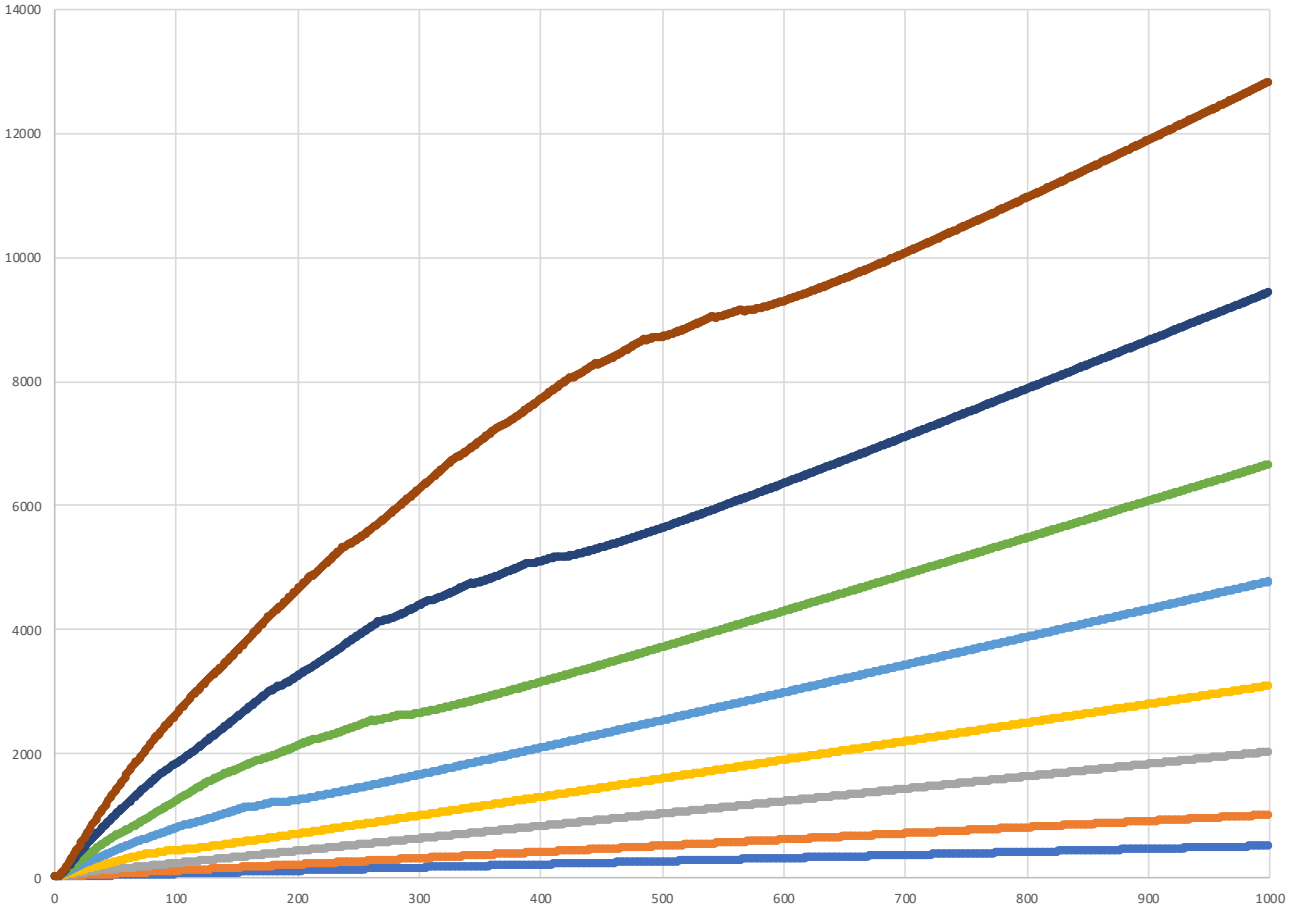


Figure 23. Calculated values of ${}^d t_{3d+k}$, $1 \leq d \leq 1000$, for $k = 3, 4, \dots, 10$ (bottom to top).

4.4 Initial segments: a glimpse of order and hope?

In the previous section we looked at the very top parts of the columns in the ${}^d t_n$ data, as shown in Tables 3 and 4. One of the most interesting/promising observations arises when one looks at the *bottom* parts of these columns.

Examining consecutive columns, one sees that the first few values at the bottom of one column are present in the next. These are the red entries in the lower parts of Tables 3 and 4, specifically the values ${}^d t_n$ with n approximately ranging from $5d$ to $6d$. Note that each column seems to add an extra number to the “Stable Column Sequence” (as we will call it), but that no extra number is added from column $d = 28$ to $d = 29$; this is indicated by green in Table 4. Although we do not have a complete explanation for why this happens, it appears that for fixed d , the last value of n for which ${}^d t_n$ is not this “stable” value is $\lceil 5.035d \rceil$; note that

$$\lceil 5.035 \cdot 28 \rceil = \lceil 140.98 \rceil = 141 \quad \text{and} \quad \lceil 5.035 \cdot 29 \rceil = \lceil 146.015 \rceil = 147,$$

so that column $d = 29$ adds an additional 6 “unstable” ${}^d t_n$ values from column $d = 28$.

In any case, the resulting Stable Column Sequence begins:

$$1, 1, 3, 6, 11, 18, 31, 47, 72, 105, 149, 206, 281, 372, 487, 627, 796, 997, 1237, 1516, 1843, 2220, 2653, 3147, \dots \quad (4.11)$$

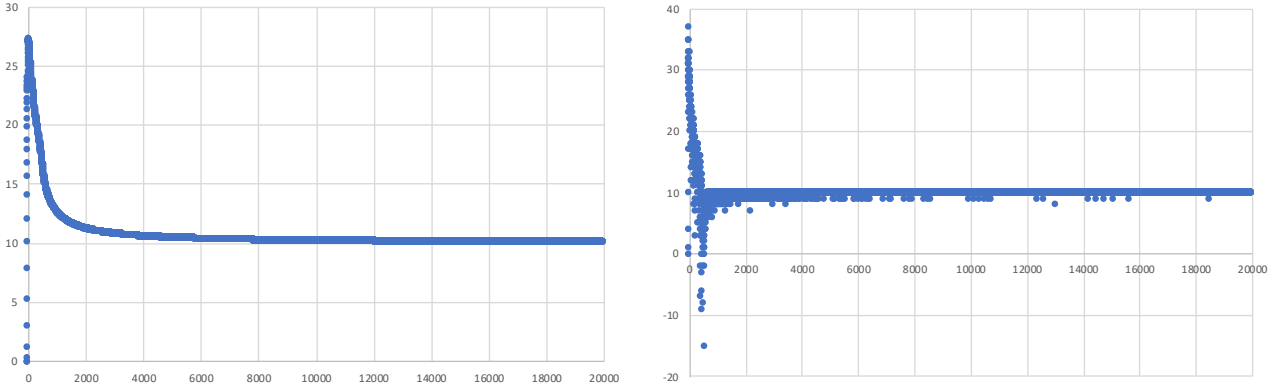


Figure 24. Left and right: calculated values of v_d/d and $v_{d+1} - v_d$, $1 \leq d \leq 20000$, where $v_d = {}^d t_{3d+10}$.

This sequence does not appear on the OEIS. The first few values are easy to understand:

- for $d \geq 1$, ${}^d t_{6d} = 1$ counts only $[(d, d), (d, d), (d, d)]$, the equilateral tetrahedron,
- for $d \geq 2$, ${}^d t_{6d-1} = 1$ counts only $[(d, d), (d, d), (d, d-1)]$,
- for $d \geq 3$, ${}^d t_{6d-2} = 3$ counts only $[(d, d), (d, d), (d, d-2)]$, $[(d, d), (d, d), (d-1, d-1)]$ and $[(d, d), (d, d-1), (d, d-1)]$.

One could similarly explain other values, with ad hoc arguments: e.g., ${}^d t_{6d-3} = 6$ for $d \geq 4$.

If we denote the sequence (4.11) by a_k ($k = 0, 1, 2, \dots$), then calculating $\left(\frac{a_{k+1}}{a_k} - 1\right) \times k$ suggests that a_k is quartic in k . Further experimentation quickly suggests the leading coefficient is $\frac{1}{96}$. Additional analysis suggests that $a_k - \frac{k^4}{96}$ is quadratic with leading coefficient $\frac{7}{16} = \frac{42}{96}$. After examining $a_k - \frac{k^4}{96} - \frac{7k^2}{16}$, it eventually appears that we have the exact formula

$$a_k = \frac{k^4 + 42k^2 + b_k}{96} \quad \text{where } b_0 = 96, \text{ and for } k \geq 1: \quad b_k = \begin{cases} 192 & \text{if } k \equiv 0 \pmod{12} \\ 53 & \text{if } k \equiv 1, 5, 7, 11 \pmod{12} \\ 104 & \text{if } k \equiv 2, 10 \pmod{12} \\ 117 & \text{if } k \equiv 3, 9 \pmod{12} \\ 128 & \text{if } k \equiv 4, 8 \pmod{12} \\ 168 & \text{if } k \equiv 6 \pmod{12}. \end{cases} \quad (4.12)$$

Equivalently, for $k \geq 1$, a_k is the nearest integer to

$$\frac{k^4 + 42k^2 + 148}{96} \quad \text{or} \quad \frac{k^4 + 42k^2 + 85}{96},$$

for even and odd k , respectively. (The values of 148 and 85 are simply the average of the maximum and minimum values of b_k for even and odd k , respectively. A single “nearest integer formula” cannot be given, unfortunately, because the distance between the maximum and minimum values of b_k for arbitrary k (i.e., $192 - 53 = 139$) is greater than the denominator, 96.) We do not currently know if there is any significance in the exact values of the numbers $b_k \in \{53, 104, 117, 128, 168, 192\}$.

Conjecture 4.13. For suitably small k (approximately $0 \leq k < d$), we have ${}^d t_{6d-k} = a_k$, where a_k is defined in (4.12). (Note then that for such k , ${}^d t_{6d-k}$ would depend only on k , and not on d .)

The formula (4.12) can be used to calculate many more values of a_k . Figure 25 plots these, together with the associated values of b_k ; the periodic nature of the latter can be readily seen in the graph.

The existence of the Stable Column Sequence implies that there are six “Stable Row Sequences”, one for each residue of n , modulo 6. So the n th row of the ${}^d t_n$ table, for suitably large n , begins:

- 18, 206, 997, 3147, 7736, 16168, 30171, 51797, 83422, ... when $n \equiv 0 \pmod{6}$,
- 11, 149, 796, 2653, 6747, 14427, 27368, 47567, 77347, ... when $n \equiv 1 \pmod{6}$,
- 6, 105, 627, 2220, 5856, 12831, 24765, 43602, 71610, ... when $n \equiv 2 \pmod{6}$,
- 3, 72, 487, 1843, 5057, 11372, 22353, 39891, 66199, ... when $n \equiv 3 \pmod{6}$,
- 1, 47, 372, 1516, 4343, 10041, 20122, 36422, 61101, ... when $n \equiv 4 \pmod{6}$,
- 1, 31, 281, 1237, 3710, 8833, 18065, 33187, 56306, ... when $n \equiv 5 \pmod{6}$.

These can all be seen in Table 4, and they are all of course subsequences of the Stable Column Sequence. None of these six (sub)sequences appear on the OEIS. Note that the (initial segments of the) Stable Row Sequences account for the left-most part of the graphs in Figures 13 and 14; see especially Figure 14, which shows values of a_k in light blue. Similarly, the Stable Column Sequence accounts for the right-most part of the graphs in Figures 15 and 16; see especially Figure 16, which shows values of a_k in light blue.

So we have seen that the first portion of a row, and the last portion of a column, in the ${}^d t_n$ table appears to be governed by a certain quartic (indeed, biquadratic) polynomial. Unfortunately, similar experimentation shows that the remainder of these rows/columns do not look at all like any polynomial. Indeed, even considering small portions at the opposite end of each row/column does not seem to yield a polynomial pattern.

A possible approach to Conjecture 4.13 might be to show that any tuple $[(A, a), (B, b), (C, c)]$ with $d = A = \max\{A, B, C, a, b, c\}$, and with perimeter greater than (around) $5.035d$, automatically satisfies conditions (T2)–(T6) from Proposition 2.5. The hope is that such a tuple is “close enough” to the equilateral $[(d, d), (d, d), (d, d)]$ that it corresponds to a tetrahedron by default. This would not immediately give the desired formula for a_k , but it would at least show that some kind of Stable Column Sequence does exist.

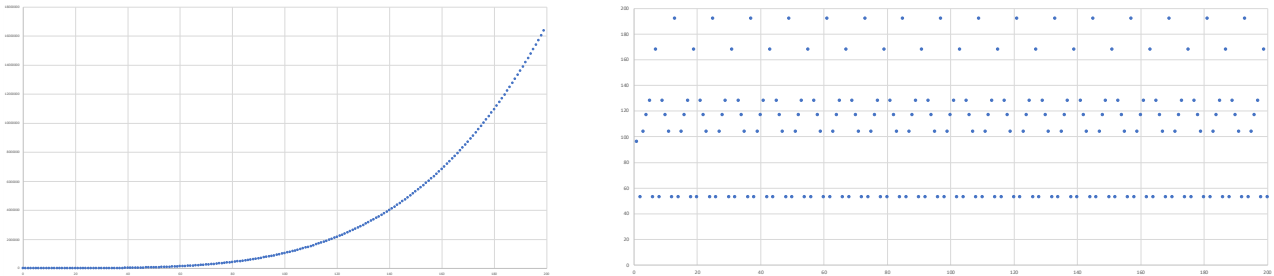


Figure 25. Calculated values of a_k (left) and b_k (right), $1 \leq k \leq 200$, as defined in (4.12).

4.5 Sums vs. maximums: more on asymptotics

We noted in Section 4.2 that one might hope to approximate values of t_n (for large n) by interpolating the ${}^d t_m$ curve (for smaller m), and using the value of $\max_d {}^d t_n$ as the scaling factor. In this section we discuss a simpler attempt to estimate t_n (and ${}^d t$) using single values of ${}^d t_n$.

To keep the following discussion manageable, it will be convenient to define a number of additional parameters:

- For fixed n we define $\mu_n = \max_d {}^d t_n$, and the ratio $\rho_n = t_n / \mu_n$.
Further, let $d^*(n)$ be the diameter corresponding to the maximum value of ${}^d t_n$: i.e., $\mu_n = {}^{d^*(n)} t_n$.

- For fixed d we define ${}^d\mu = \max_n {}^d t_n$, and the ratio ${}^d\rho = {}^d t / {}^d\mu$.

Further, let $n^*(d)$ be the perimeter corresponding to the maximum value of ${}^d t_n$: i.e., ${}^d\mu = {}^d t_{n^*(d)}$.

Computationally, it seems that

$$d^*(n) \approx 0.238n \approx \frac{n}{4.2} \quad \text{and} \quad n^*(d) \approx 4.5d. \quad (4.14)$$

We do not currently understand the significance of the number $0.238 \approx \frac{1}{4.2}$. However, $4.5d$ is of course almost exactly mid-way between the extreme values of $3d + 3 \leq n \leq 6d$; cf. Lemma 3.2. These values of $d^*(n)$ and $n^*(d)$ can be seen by locating the peaks in Figures 13–16.

Figure 26 shows graphs of calculated values of ρ_n ($n \leq 2000$) and ${}^d\rho$ ($d \leq 300$). These graphs strongly suggest that (at least approximately) ρ_n is linear in n , and ${}^d\rho$ is linear in d , so it seems worthwhile to look at the values of ρ_n/n and ${}^d\rho/d$. Accordingly,

- Table 7 shows calculated values of t_n , μ_n , ρ_n and ρ_n/n (as well as $d^*(n)$), and
- Table 8 shows calculated values of ${}^d t$, ${}^d\mu$, ${}^d\rho$ and ${}^d\rho/d$ (as well as $n^*(d)$).

Note that we have been able to calculate μ_n and ${}^d\mu$ for higher values of n and d than for t_n and ${}^d t$. To obtain these we used the approximations for $d^*(n)$ and $n^*(d)$ from (4.14), and calculated enough values of ${}^d t_n$ around the critical values, to ensure that we had found the peak of the curve. For the round values of n and d we used, the approximations in (4.14) were in fact exact, with a single exception: $n^*(1900) = 8551$, whereas $4.5 \cdot 1900 = 8550$. But here we note that

- ${}^{1900}t_{8549} = 287666266084$,
- ${}^{1900}t_{8550} = 287666506644 = {}^{1900}t_{8549} + 240560$,
- ${}^{1900}t_{8551} = 287666521356 = {}^{1900}t_{8550} + 14712$,
- ${}^{1900}t_{8552} = 287666235410 = {}^{1900}t_{8551} + 271234$,

meaning that ${}^{1900}t_{8550}$ is comparatively very close to the maximum value of ${}^{1900}\mu = {}^{1900}t_{8551}$.

The values displayed in Tables 7 and 8 strongly suggest that ρ_n/n and ${}^d\rho/d$ tend to limits of around 0.07122 and 1.1657, respectively, leading to asymptotic expressions:

$$\rho_n \sim 0.07122n \quad \text{as } n \rightarrow \infty \quad \text{and} \quad {}^d\rho \sim 1.1657d \quad \text{as } d \rightarrow \infty. \quad (4.15)$$

(Interestingly, 0.07122 is quite close to $\frac{1}{14}$, although computational evidence suggests that the limit $\lim_{n \rightarrow \infty} \frac{\rho_n}{n}$ is around $\frac{1}{14.041}$, and this can make quite a big difference in the calculations that follow.)

By definition, we have $t_n = \rho_n \times \mu_n$ and ${}^d t = {}^d\rho \times {}^d\mu$. Thus, if we could also obtain asymptotic expressions for μ_n and ${}^d\mu$, then these could be combined with (4.15) to yield asymptotic expressions for t_n and ${}^d t$ themselves (cf. Conjecture 4.1 and Remark 4.3).

Calculations show that the ratios $\left(\frac{\mu_{n+1}}{\mu_n} - 1\right) \times n$ and $\left(\frac{{}^{d+1}\mu}{{}^d\mu} - 1\right) \times d$ both seem to approach 4, suggesting that $\mu_n \sim \frac{n^4}{D}$ and ${}^d\mu \sim \frac{d^4}{E}$ for some constants D and E . Tables 7 and 8 also show values of $D_n = \frac{n^4}{\mu_n}$ and ${}^d D = \frac{d^4}{{}^d\mu}$, respectively. (These tables also give values of $C_n = \frac{n^5}{t_n}$ and ${}^d C = \frac{d^5}{{}^d t}$.) These seem to approach limits of around $D_n \rightarrow 16310.5$ and ${}^d D \rightarrow 45.301$, respectively.

Putting all of the above together, we have (very approximate) candidates for asymptotic formulas:

$$t_n = \rho_n \times \mu_n \sim 0.07122n \times \frac{n^4}{16310.5} \approx \frac{n^5}{229016} \quad \text{as } n \rightarrow \infty \quad (4.16)$$

$$\text{and} \quad {}^d t = {}^d\rho \times {}^d\mu \sim 1.1657d \times \frac{d^4}{45.301} \approx \frac{d^5}{38.86} \quad \text{as } d \rightarrow \infty. \quad (4.17)$$

Note that (4.16) and (4.17) are reasonably close to Conjecture 4.1 and (4.4). We should stress, however, that in the above discussion we often rounded off certain numbers to seemingly-arbitrary precision. Thus, the asymptotic expressions in (4.16) and (4.17) are very speculative, and are not meant to be exact predictions.

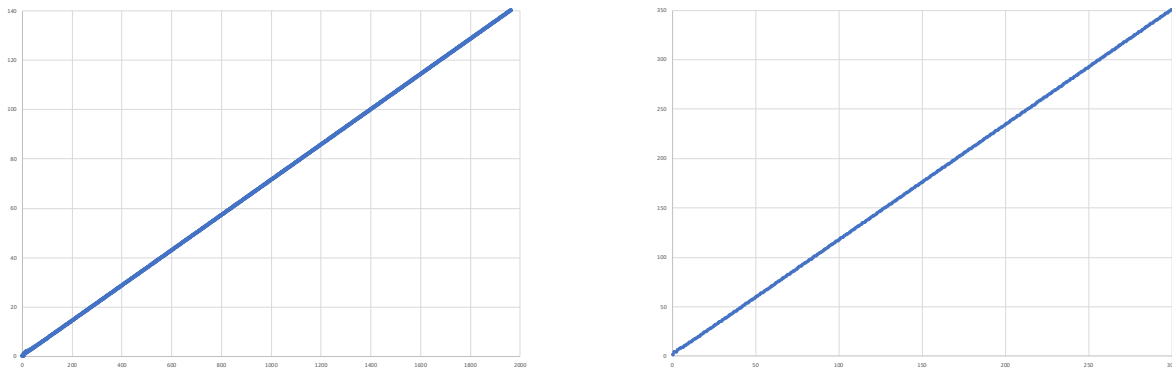


Figure 26. Calculated values of ρ_n (left), $1 \leq n \leq 2000$, and ${}^d\rho$ (right), $1 \leq d \leq 300$; see Section 4.5 for more details.

5 Conclusion

Enumeration of integer triangles of given perimeter is a classical problem [8, 11], and polygons have recently been treated as well [4]. The current article considered the corresponding problem for tetrahedra, which is considerably more difficult. The central theme is the calculation of the numbers t_n , ${}^d t$ and ${}^d t_n$ of integer tetrahedra with perimeter n and/or diameter d (as appropriate), up to congruence. In Section 2 we set up a framework in which these numbers could (in principle) be calculated via an application of Burnside’s Lemma, and made some partial progress by finding explicit formulas for some of the relevant fix-set parameters. The complexity of the other parameters—and of the numbers t_n , ${}^d t$ and ${}^d t_n$ themselves—is highlighted by the computations discussed in Section 3, and is visible in many of the figures therein. Nevertheless, a number of apparent patterns emerged from an exploration of the data. Several of these were discussed in Section 4, which contains a number of conjectures and avenues for future exploration; we hope that future studies will shed further light on the situation.

References

- [1] The on-line encyclopedia of integer sequences. Published electronically at <http://oeis.org/>.
- [2] P. J. Cameron. *Combinatorics: topics, techniques, algorithms*. Cambridge University Press, Cambridge, 1994.
- [3] J. East, M. Hendriksen, and L. Park. *On the enumeration of integer tetrahedra: supplemental data*, 2021, https://staff.cdm.s.westernsydney.edu.au/~lapark/integer_tetrahedra/.
- [4] J. East and R. Niles. Integer polygons of given perimeter. *Bull. Aust. Math. Soc.*, 100(1):131–147, 2019.
- [5] J. East and R. Niles. Integer triangles of given perimeter: a new approach via group theory. *Amer. Math. Monthly*, 126(8):735–739, 2019.
- [6] M. D. Hirschhorn. Triangles with integer sides, revisited. *Math. Mag.*, 73(1):53–56, 2000.
- [7] M. D. Hirschhorn. Triangles with integer sides. *Math. Mag.*, 76(4):306–308, 2003.
- [8] R. Honsberger. *Mathematical gems. III*, volume 9 of *The Dolciani Mathematical Expositions*. Mathematical Association of America, Washington, DC, 1985.
- [9] J. E. Humphreys. *Reflection groups and Coxeter groups*, volume 29 of *Cambridge Studies in Advanced Mathematics*. Cambridge University Press, Cambridge, 1990.
- [10] T. Jenkyns and E. Muller. Triangular triples from ceilings to floors. *Amer. Math. Monthly*, 107(7):634–639, 2000.
- [11] J. H. Jordan, R. Walch, and R. J. Wisner. Triangles with integer sides. *Amer. Math. Monthly*, 86(8):686–689, 1979.
- [12] S. Kurz. Enumeration of integral tetrahedra. *J. Integer Seq.*, 10(9):Article 07.9.3, 12, 2007.
- [13] K. Menger. Untersuchungen über allgemeine Metrik. *Math. Ann.*, 100(1):75–163, 1928.
- [14] K. Wirth and A. S. Dreiding. Edge lengths determining tetrahedrons. *Elem. Math.*, 64(4):160–170, 2009.

1	0	41	492	81	14903	121	111246	161	466128
2	0	42	568	82	15790	122	116006	162	480898
3	0	43	630	83	16811	123	120768	163	495924
4	0	44	702	84	17854	124	125837	164	511275
5	0	45	797	85	18940	125	130985	165	527179
6	1	46	884	86	20107	126	136402	166	543486
7	0	47	977	87	21261	127	141853	167	559950
8	0	48	1089	88	22511	128	147575	168	576987
9	1	49	1217	89	23831	129	153500	169	594453
10	1	50	1338	90	25251	130	159470	170	612306
11	1	51	1469	91	26631	131	165757	171	630619
12	3	52	1624	92	28173	132	172253	172	649344
13	2	53	1771	93	29744	133	178772	173	668273
14	3	54	1970	94	31341	134	185682	174	688082
15	6	55	2146	95	33116	135	192674	175	708017
16	6	56	2343	96	34849	136	200070	176	728557
17	7	57	2579	97	36696	137	207440	177	749759
18	12	58	2782	98	38695	138	215111	178	770893
19	11	59	3042	99	40619	139	223151	179	792983
20	18	60	3322	100	42817	140	231179	180	815666
21	21	61	3586	101	44951	141	239687	181	838151
22	25	62	3912	102	47257	142	248292	182	862084
23	31	63	4221	103	49641	143	257130	183	885874
24	38	64	4568	104	52008	144	266522	184	910270
25	46	65	4953	105	54685	145	275691	185	935691
26	56	66	5339	106	57310	146	285536	186	960959
27	66	67	5731	107	60046	147	295385	187	987344
28	76	68	6204	108	62944	148	305605	188	1014149
29	90	69	6657	109	65896	149	316146	189	1041441
30	117	70	7169	110	69029	150	326952	190	1069393
31	123	71	7683	111	72152	151	337891	191	1097727
32	151	72	8230	112	75549	152	349316	192	1127002
33	175	73	8857	113	78976	153	361051	193	1156747
34	196	74	9446	114	82574	154	372976	194	1186965
35	234	75	10095	115	86199	155	385325	195	1217963
36	264	76	10846	116	90052	156	398032	196	1249657
37	297	77	11513	117	94053	157	410750	197	1281804
38	346	78	12345	118	98089	158	424249	198	1314840
39	391	79	13125	119	102371	159	437744	199	1348514
40	448	80	13969	120	106711	160	451759	200	1382630

Table 1. Calculated values of t_n .

100	42817
200	1382630
300	10542791
400	44512930
500	135995968
600	338647149
700	732301457
800	1428244253
900	2574424362
1000	4360687860
1100	7024066455
1200	10853927088
1300	16197354205
1400	23464200340
1500	33132516713
1600	45753651322
1700	61957547844
1800	82458026396
1900	10805787719
2000	139654346301

2100	178244109766
2200	224928623704
2300	280919515766
2400	347543441363
2500	426247856357
2600	518605683615
2700	626321040933
2800	751234199645
2900	895326815879
3000	1060727392377
3100	1249716260424
3200	1464730980692
3300	1708371608956
3400	1983405792552
3500	2292773954230
3600	2639594896693
3700	3027170849616
3800	3458992238494
3900	3938743901688
4000	4470309160343

4100	5057776483155
4200	5705443122022
4300	6417821623924
4400	7199644279518
4500	8055868989730
4600	8991684402358
4700	10012513881131
4800	11124023171269
4900	12332123259033
5000	13642977397892
5100	15063004902111
5200	16598887173873
5300	18257573582602
5400	20046284952842
5500	21972520100932
5600	24044061595649
5700	26268978527115
5800	28655635295636
5900	31212693377826
6000	33949118928429

6100	36874187631384
6200	39997488181501
6300	43328930438429
6400	46878747743940
6500	50657504819100
6600	54676100750626
6700	58945775513454
6800	63478115036529
6900	68285056161851
7000	73378891579018
7100	78772276600831
7200	84478231957643
7300	90510152207309
7400	96881807240927
7500	103607350139966
7600	110701321888040
7700	118178657158659
7800	126054687371188
7900	134345147515787
8000	143066182224551

8100	152234350689174
8200	161866628410449
8300	171980417994570
8400	182593551239230
8500	193724293506541
8600	205391352861569
8700	217613878464370
8800	230411473926234
8900	243804197732022
9000	257812568218126
9100	272457573348976
9200	287760666512263
9300	303743784383639
9400	320429342544289
9500	337840242823660
9600	355999882739690
9700	374932153990010
9800	394661455344190
9900	415212690326932
10000	436611276762080

Table 2. Calculated values of t_n .

n/d	1	2	3	4	5	6	7	8	9	10	11	12	13	14	15
6	1
7
8
9	.	1
10	.	1
11	.	1
12	.	1	2
13	.	.	2
14	.	.	3
15	.	.	4	2
16	.	.	3	3
17	.	.	1	6
18	.	.	1	8	3
19	.	.	.	7	4
20	.	.	.	8	10
21	.	.	.	6	12	3
22	.	.	.	3	17	5
23	.	.	.	1	17	13
24	.	.	.	1	16	17	4
25	15	25	6
26	11	29	16
27	6	34	22	4
28	3	32	34	7
29	1	29	41	19
30	1	27	55	29	5
31	18	55	42	8
32	11	61	57	22
33	6	57	72	35	5
34	3	51	81	52	9
35	1	43	94	71	25
36	1	31	95	91	40	6
37	18	100	109	60	10
38	11	90	130	87	28
39	6	81	140	111	47	6	.	.	.
40	3	67	155	141	71	11	.	.	.
41	1	47	149	163	101	31	.	.	.
42	1	31	153	192	132	52	7	.	.
43	18	138	209	172	81	12	.	.
44	11	121	221	200	115	34	.	.
45	6	100	231	239	158	56	7	.
46	3	72	229	271	202	94	13	.
47	1	47	224	296	242	130	37	.
48	1	31	200	320	289	180	60	8
49	18	175	331	342	233	104	14
50	11	143	337	374	288	145	40

Table 3. Calculated values of d_t^n .

n	(i)	(ii)	(iii)	(iv)	(v)	t_n	t'_n
1	0	0	0	0	0	0	0
2	0	0	0	0	0	0	0
3	0	0	0	0	0	0	0
4	0	0	0	0	0	0	0
5	0	0	0	0	0	0	0
6	1	1	1	1	1	1	1
7	0	0	0	0	0	0	0
8	0	0	0	0	0	0	0
9	4	1	0	2	0	1	1
10	3	0	3	1	1	1	1
11	6	0	2	2	0	1	1
12	11	2	3	5	1	3	3
13	18	0	2	4	0	2	2
14	27	0	3	5	1	3	3
15	42	3	6	10	0	6	7
16	57	0	9	9	1	6	7
17	84	0	8	10	0	7	9
18	120	3	8	18	2	12	14
19	138	0	6	18	0	11	13
20	234	0	18	22	2	18	24
21	268	4	12	28	0	21	28
22	354	0	18	30	2	25	34
23	480	0	16	36	0	31	44
24	560	5	16	42	2	38	54
25	750	0	26	46	0	46	69
26	897	0	33	55	3	56	83
27	1082	5	30	62	0	66	101
28	1326	0	30	66	2	76	118
29	1584	0	36	78	0	90	141
30	2013	6	57	93	3	117	186
31	2256	0	48	92	0	123	200
32	2811	0	51	107	3	151	247
33	3258	6	50	124	0	175	288
34	3738	0	66	124	4	196	328
35	4554	0	70	142	0	234	397
36	5047	7	83	161	3	264	446
37	5886	0	78	168	0	297	510
38	6942	0	78	184	4	346	598
39	7778	8	98	208	0	391	678
40	9048	0	120	220	4	448	784
41	10104	0	108	230	0	492	869
42	11648	8	112	260	4	568	1004
43	13086	0	122	278	0	630	1121
44	14652	0	144	290	4	702	1257
45	16698	9	146	320	0	797	1434
46	18609	0	165	347	5	884	1592
47	20778	0	162	364	0	977	1772
48	23170	10	174	390	4	1089	1981
49	26118	0	190	420	0	1217	2224
50	28755	0	219	445	5	1338	2451
51	31696	10	216	472	0	1469	2702
52	35265	0	225	501	5	1624	2995
53	38616	0	232	532	0	1771	3276
54	42950	11	266	568	6	1970	3653
55	47136	0	272	592	0	2146	3996
56	51519	0	291	635	5	2343	4366
57	56838	12	302	676	0	2579	4820
58	61590	0	330	692	6	2782	5215
59	67524	0	340	744	0	3042	5712
60	73716	12	364	798	6	3322	6242
61	80058	0	366	818	0	3586	6763
62	87486	0	390	866	6	3912	7388
63	94438	13	406	924	0	4221	7980
64	102546	0	438	956	6	4568	8655
65	111510	0	454	1000	0	4953	9406
66	120217	13	465	1063	7	5339	10143
67	129474	0	478	1106	0	5731	10909
68	140337	0	537	1151	7	6204	11829
69	150746	14	542	1214	0	6657	12707
70	162687	0	579	1265	7	7169	13702
71	174732	0	580	1320	0	7683	14706
72	187293	15	593	1381	7	8230	15766
73	201954	0	646	1446	0	8857	16991
74	215556	0	696	1502	8	9446	18137
75	230754	15	690	1556	0	10095	19412
76	248271	0	723	1637	7	10846	20870
77	263898	0	734	1702	0	11513	22175
78	283060	16	808	1770	8	12345	23801
79	301542	0	806	1840	0	13125	25330
80	321228	0	840	1910	8	13969	26979
81	342986	17	870	1990	0	14903	28811
82	363870	0	906	2054	8	15790	30549
83	387786	0	946	2140	0	16811	32552
84	411902	17	990	2240	8	17854	34584
85	437766	0	1010	2294	0	18940	36733
86	465111	0	1035	2383	9	20107	39018
87	491910	18	1086	2492	0	21261	41276
88	521439	0	1143	2557	9	22511	43739
89	552630	0	1146	2646	0	23831	46339
90	585595	19	1211	2765	9	25251	49115
91	618420	0	1232	2838	0	26631	51843
92	654549	0	1317	2933	9	28173	54875
93	691444	19	1328	3046	0	29744	57965
94	729144	0	1380	3140	10	31341	61107
95	771042	0	1422	3246	0	33116	64609
96	811697	20	1453	3351	9	34849	68018
97	855402	0	1522	3456	0	36696	71664
98	902544	0	1560	3566	10	38695	75602
99	947912	20	1592	3668	0	40619	79404
100	999738	0	1674	3798	10	42817	83730

Table 5. Calculated values of $\text{fix}(\sigma)$, for σ of types (i)–(v), as well as t_n and t'_n .

n	C_n	d_n	r_n
100	233552.094		
200	231442.975	-2109.119	
300	230489.251	-953.724	0.452
400	230045.517	-443.734	0.465
500	229786.224	-259.293	0.584
600	229619.532	-166.692	0.643
700	229509.307	-110.225	0.661
800	229428.544	-80.763	0.733
900	229367.780	-60.765	0.752
1000	229321.619	-46.161	0.760
1100	229284.562	-37.057	0.803
1200	229255.271	-29.291	0.790
1300	229230.648	-24.623	0.841
1400	229210.453	-20.195	0.820
1500	229193.275	-17.179	0.851
1600	229178.649	-14.625	0.851
1700	229166.106	-12.543	0.858
1800	229155.133	-10.973	0.875
1900	229145.626	-9.507	0.866
2000	229137.158	-8.468	0.891
2100	229129.647	-7.511	0.887
2200	229122.995	-6.652	0.886
2300	229116.976	-6.019	0.905
2400	229111.617	-5.359	0.890
2500	229106.724	-4.893	0.913
2600	229102.310	-4.414	0.902
2700	229098.275	-4.035	0.914
2800	229094.575	-3.699	0.917
2900	229091.195	-3.381	0.914
3000	229088.078	-3.116	0.922
3100	229085.208	-2.870	0.921
3200	229082.558	-2.650	0.923
3300	229080.095	-2.463	0.929
3400	229077.802	-2.292	0.931
3500	229075.679	-2.123	0.926
3600	229073.696	-1.982	0.934
3700	229071.831	-1.865	0.941
3800	229070.095	-1.736	0.931
3900	229068.457	-1.637	0.943
4000	229066.931	-1.526	0.932
4100	229065.482	-1.449	0.949
4200	229064.122	-1.360	0.939
4300	229062.837	-1.285	0.945
4400	229061.628	-1.209	0.941
4500	229060.484	-1.144	0.946
4600	229059.392	-1.092	0.955
4700	229058.366	-1.026	0.939
4800	229057.387	-0.979	0.955
4900	229056.459	-0.928	0.947
5000	229055.573	-0.887	0.956
5100	229054.729	-0.843	0.951
5200	229053.929	-0.801	0.949
5300	229053.160	-0.768	0.960
5400	229052.428	-0.732	0.953
5500	229051.730	-0.698	0.952
5600	229051.059	-0.672	0.963
5700	229050.420	-0.638	0.950
5800	229049.805	-0.615	0.964
5900	229049.217	-0.588	0.956
6000	229048.654	-0.563	0.958
6100	229048.111	-0.543	0.965
6200	229047.591	-0.520	0.956
6300	229047.090	-0.501	0.965
6400	229046.610	-0.480	0.958
6500	229046.146	-0.464	0.965
6600	229045.700	-0.446	0.963
6700	229045.270	-0.430	0.963
6800	229044.855	-0.415	0.965
6900	229044.455	-0.400	0.965
7000	229044.070	-0.385	0.962
7100	229043.698	-0.373	0.968
7200	229043.339	-0.359	0.963
7300	229042.990	-0.349	0.972
7400	229042.654	-0.337	0.966
7500	229042.329	-0.325	0.966
7600	229042.014	-0.314	0.967
7700	229041.709	-0.306	0.972
7800	229041.413	-0.296	0.968
7900	229041.127	-0.286	0.966
8000	229040.850	-0.277	0.969
8100	229040.580	-0.270	0.975
8200	229040.320	-0.261	0.965
8300	229040.067	-0.253	0.971
8400	229039.821	-0.246	0.973
8500	229039.582	-0.239	0.969
8600	229039.349	-0.233	0.978
8700	229039.124	-0.225	0.966
8800	229038.905	-0.219	0.972
8900	229038.692	-0.213	0.974
9000	229038.485	-0.207	0.970
9100	229038.282	-0.203	0.981
9200	229038.086	-0.196	0.965
9300	229037.895	-0.191	0.977
9400	229037.708	-0.187	0.975
9500	229037.527	-0.181	0.970
9600	229037.350	-0.177	0.977
9700	229037.178	-0.172	0.971
9800	229037.010	-0.168	0.979
9900	229036.846	-0.164	0.975
10000	229036.686	-0.160	0.974

Table 6. Calculated values of $C_n = n^5/t_n$, and associated differences $d_n = C_n - C_{n-100}$ and ratios $r_n = d_n/d_{n-100}$; see Section 4.1 for more details.

n	$d^*(n)$	t_n	μ_n	ρ_n	ρ_n/n	D_n	C_n
1000	238	4360687860	61261647	71.181368	0.071181368	16323.42663	229321.6190
2000	476	139654346301	980662960	142.408097	0.071204049	16315.49335	229137.1579
3000	714	1060727392377	4965253737	213.630048	0.071210016	16313.36570	229088.0784
4000	952	4470309160343	15693529026	284.850473	0.071212618	16312.45589	229066.9310
5000	1190	13642977397892	38315438250	356.069982	0.071213996	16311.96271	229055.5726
6000	1428	33949118928429	79452345303	427.289072	0.071214845	16311.66450	229048.6541
7000	1666	73378891579018	147197080983	498.507790	0.071215399	16311.46477	229044.0703
8000	1904	143066182224551	251113882084	569.726297	0.071215787	16311.32443	229040.8501
9000	2142	257812568218126	402238432945	640.944641	0.071216071	16311.22106	229038.4849
10000	2380	436611276762080	613077830990	712.162885	0.071216288	16311.14272	229036.6862
11000	2618	703171140799375	897610575535	783.381079	0.071216462	16311.08233	229035.2813
12000	2856	1086440561201385	1271286727639	854.599153	0.071216596	16311.03318	229034.1588
13000	3094	1621131464654093	1751027590016	925.817202	0.071216708	16310.99371	229033.2450
14000	3332	2348243259709892	2355226146934	997.035152	0.071216797	16310.96022	229032.4896
15000	3570	3315586803814407	3103746427345	1068.253120	0.071216875	16310.93299	229031.8562
16000	3808	4578308347767338	4017924323570	1139.471025	0.071216939	16310.90950	229031.3191
17000	4046	6199413506818430	5120566904917	1210.688899	0.071216994	16310.88931	229030.8589
18000	4284	8250291212969114	6435952631653	1281.906764	0.071217042	16310.87207	229030.4610
19000	4522	10811237680756863	7989831502801	1353.124616	0.071217085	16310.85711	229030.1141
20000	4760	13971980347794463	9809425098449	1424.342427	0.071217121	16310.84374	229029.8097
30000	7140		49660446083302			16310.76770	
40000	9520		156951842767924			16310.78743	

Table 7. Calculated values of t_n and associated numbers defined in Section 4.5.

d	$n^*(d)$	${}^d t$	${}^d \mu$	${}^d \rho$	${}^d \rho/d$	${}^d D$	${}^d C$
100	450	256866619	2205518	116.465438	1.164654376	45.34082243	38.93071057
200	900	8227353208	35302466	233.053215	1.165266076	45.32261287	38.89464715
300	1350	62496428392	178753878	349.622784	1.165409278	45.31370223	38.88222195
400	1800	263399396125	564995595	466.197256	1.165493140	45.31008777	38.87632299
500	2250	803900006590	1379446698	582.769894	1.165539789	45.30802103	38.87299383
600	2700	2000468396580	2860504080	699.341214	1.165568690	45.30669993	38.87089650
700	3150	4323958989350	5299548768	815.910784	1.165586834	45.30574404	38.86947134
800	3600	8430487428682	9040920238	932.481120	1.165601400	45.30512262	38.86845248
900	4050	15192308794063	14481975268	1049.049492	1.165610546	45.30459332	38.86769338
1000	4500	25728695195597	22072986511	1165.619124	1.165619124	45.30424551	38.86710898
1100	4950	41436812404716	32317280628	1282.187474	1.165624976	45.30393559	38.86664795
1200	5400	64022597756042	45771110797	1398.755605	1.165629670	45.30368531	38.86627671
1300	5850	95531638650235	63043701776	1515.324068	1.165633899	45.30349455	38.86597207
1400	6300	138380047521949	84797295248	1631.892233	1.165637310	45.30333177	38.86571870
1500	6750	195385341804382	111747102464	1748.460027	1.165640018	45.30318808	38.86550511
1600	7200	269797320709960	144661271196	1865.027996	1.165642497	45.30307211	38.86532295
1700	7650	365328940733369	184360988174	1981.595696	1.165644527	45.30296828	38.86516620
1800	8100	486187194335920	231720360895	2098.163461	1.165646367	45.30288128	38.86503022
1900	8551	637103991780086	287666521356	2214.731102	1.165647948	45.30280388	38.86491110
2000	9000	823367026746276	353179561833	2331.298625	1.165649312	45.30273472	38.86480629
3000	13501		1787987440725			45.30233164	
4000	18001		5650944679691			45.30215999	
5000	22501		13796279726716			45.30206783	
6000	27001		28608001167605			45.30201157	
7000	31502		52999897734423			45.30197420	

Table 8. Calculated values of ${}^d t$ and associated numbers defined in Section 4.5.